THE UNIVERSITY OF ALBERTA

RELEASE FORM

NAME OF AUTHOR Santosh Singh Sikerwar

TITLE OF THESIS **STRUCTURAL STUDIES ON THE GAP JUNCTIONS FROM MOUSE LIVER: ISOLATION AND CHARACTERIZATION**

DEGREE FOR WHICH THESIS WAS PRESENTED **DOCTOR OF PHILOSOPHY**

YEAR THIS DEGREE GRANTED FALL 1983

THE UNIVERSITY OF ALBERTA

STRUCTURAL STUDIES ON THE GAP JUNCTIONS FROM MOUSE LIVER: ISOLATION AND CHARACTERIZATION

by

Santosh Singh Sikerwar

A THESIS

SUBMITTED TO THE FACULTY OF GRADUATE STUDIES AND RESEARCH

IN PARTIAL FULFILMENT OF THE REQUIREMENTS FOR THE DEGREE

OF DOCTOR OF PHILOSOPHY

IN

CELL BIOLOGY

Zoology

EDMONTON, ALBERTA

FALL 1983

THE UNIVERSITY OF ALBERTA

FACULTY OF GRADUATE STUDIES AND RESEARCH

The undersigned certify that they have read, and recommend to the Faculty of Graduate Studies and Research, for acceptance, a thesis entitled **STRUCTURAL STUDIES ON THE GAP JUNCTIONS FROM MOUSE LIVER: ISOLATION AND CHARACTERIZATION** submitted by Santosh Singh Sikerwar in partial fulfilment of the requirements for the degree of DOCTOR OF PHILOSOPHY in CELL BIOLOGY.

In the memory of my father

(Shree Hari Singh Sikerwar)

ABSTRACT

This thesis concerns the structure and characterization of the gap junctions in mouse liver. In most eukaryotic organized tissues in animals, the cell surface is differentiated at the intercellular contacts (gap junctions) to provide communicating channels which regulate the passage of metabolically important ions and small molecules between the apposing cells. This mode of cell-to-cell communication has important implications in the regulation of cell-growth, development and differentiation. The polypeptide composition of the gap junctions is as yet uncertain because investigations of the polypeptides are complicated by the endogenous and exogenous proteolysis and a marked propensity of the gap-junctional polypeptide(s) to aggregate in the presence of sodium-dodecyl sulphate (SDS). This has resulted in the apparent heterogeneity in the reported polypeptide composition. Furthermore, the gap junctions isolated by the conventional methods usually display a high degree of mosaicity and/or short-range disorder which has been restrictive in the resolutions attained in the structural studies thus far (up to approximately 1.8 nm).

Therefore, a new method that aims at minimizing proteolysis has been developed to isolate the gap junctions from mouse liver. This method employs the solubilization of the plasma membranes by an anionic detergent, n-dodecanoyl sarcosine in combination with non-ionic polyoxyethylene alcohol detergents (Brij 35 and Brij 58) and a polyoxyethylene ether detergent (W-1). Purified gap junctions have been isolated by centrifugation in a sucrose gradient containing 1-O-n-octyl-β-(D)

glucopyranoside. The polypeptide composition of these junctions has been resolved by sodium dodecyl sulphate polyacrylamide gel (SDS-PAGE) electrophoresis, which reveals a single major component of 26,000 Mr. The purified gap junctions are in the form of plaques of various shapes and sizes with lateral dimensions as large as approximately 1 μm. Characterization of these junctions by electron microscopy (involving optical diffraction analysis of the micrographs of negatively stained specimen) and X-ray diffraction has unravelled the presence of an hexagonal lattice of connexons with the lattice constant of approximately 7.6-8.4 nm.

Since the gap junctional coupling is quite susceptible to perturbations in the intracellular milieu, it has been suggested that the isolation procedures uncouple the gap junctions and induce the connexons to pack tightly in two-dimensional hexagonal arrays. Therefore, in the present work in situ substructure of connexons (in mouse liver) has been resolved by employing rapid freezing (which bypasses cryoprotection and chemical fixation), freeze-etching and rotary shadowing, in conjunction with Markham's rotational integration technique for contrast enhancement. Some connexons appear to have six subunits enclosing a central depression which corresponds to the putative aqueous channel while the rest reveal less than six subunits. Visualization of less than six subunits may be due to local variations in the angle of shadowing because of an uneven plane of fracturing and/or plastic deformation. Using Markham's rotational integration technique, models of connexons and tilting experiments with the replicas, it has been found that these apparent deviations from the hexameric symmetry could result from the inclination of the fractured face relative to the plane of viewing.

In the past, freeze fracturing employing conventional chemical fixation (with glutaraldehyde) and cryoprotective treatment has been used extensively to characterize the structural changes in gap junctions induced upon uncoupling treatment. Since glutaraldehyde is known to uncouple the cells it remained to be determined if the glutaraladehyde fixation itself causes any structural change in the gap junctions. Rapid freezing (without prior cryoprotection and chemical fixation) has permitted the elaboration of structural alterations in gap junctions. Glutaraldehyde fixation reduces the average interconnexon spacing from 10 ± 2 nm in unfixed preparations to 9 ± 2 nm in the fixed preparations. The fixed, glycerinated and conventionally frozen preparations display an average interconnexon spacing of 9 ± 2 nm. In the light of well-known cross-linking and denaturing properties of glutaraldehyde it has been suggested that fixation perhaps results in conformational alterations in the connexons leading to a contraction of the gap junctional lattice. Based upon these results, the structural correlates of glutaraldehyde induced uncoupling are presumably different from the ones induced by functional uncouplers such as the free cytoplasmic concentrations of Ca^{2+} and/or H^{+} ions.

ACKNOWLEDGEMENTS

I am greatly indebted to Dr. S.K. Malhotra for his encouragement, guidance, assistance and patience in the completion of this project.

I owe a special debt of gratitude to Dr. P.N.T. Unwin who has been a constant source of inspiration and insight. I am thankful to him for his generous hospitality during my stay at Stanford. I am also indebted to Peter Ennis for his help with the x-ray diffraction experiments.

I must also acknowledge my indebtedness to Dr. R.F. Egerton. I have benefited myself immensely from frequent discussion with him.

I am thankful to the members of my supervisory committee (Dr. F.S. Chia amd Dr. E.A. Cossins) for critically reading the thesis.

I am grateful to the department of Zoology and Alberta Heritage Foundation for Medical Research for supporting me during the course of this work. I also wish to thank Sanjay Pimpilikar for his help in carrying out the electrophoresis experiments.

I am deeply indebted to Manoj Misra for his friendship. He provided answers to my mathematical enquiries ranging from embarassingly naive to embarassingly sophisticated ones.

Finally, I am deeply grateful to my family for their wholehearted support and especially to my wife Meenu whose love and affection transcended the geographical distances between us and sustained my academic indulgence.

TABLE OF CONTENTS

Page

LIST OF FIGURES AND PHOTOGRAPHIC PLATES

NOMENCLATURE

Equivalent Terms: Electrotonic Synapse, Electrotonic Junction, Nexus, Macula Communicans, Gap Junction, Intercellular Communicating Junction, Cell-to-Cell Communicating Junction and Electrical Synapse.

CHEMICALS

All the chemicals used were purchased from Sigma Chemical Company (St. Louis, MO 63178, USA) unless noted otherwise.

1. INTRODUCTION

1.1 Significance of Gap Junctions and Outstanding Problems

Gap junctions are commonly regarded as the plasma membrane specializations that provide low-resistance hydrophilic passages between the apposed cells in organized tissues throughout the animal kingdom (Gilula, 1979). These permeable junctions provide through the large hydrophilic intercellular channels, a mechanism for the equilibration of ions and small cytoplasmic molecules in a coupled cell ensemble. By using fluorescent tracers it has been shown that the gap junctions allow the passage of ions and small molecules (up to a molecular weight of approximately 1200) from one cell to the other (Loewenstein, 1981). They mediate electrical coupling in excitable tissues such as the myocardium (where they are morphologically represented as the intercalated discs) and nervous system where they comprise the electrotonic synapses (Bennett, 1977). This mode of direct cell-to-cell communication has profound implications for regulating and synchronizing the cell activities in tissues. Also, it has been suggested that the gap junctions may be involved in regulating the diffusible intercellular signals responsible for differentiation and controlled growth (Crick, 1970; Loewenstein, 1979; Bennett et al., 1981; Wolpert, 1981; Gierer, 1981). The precise mechanism of such a regulation is still unclear. There is also some evidence from in vitro studies on the heterologous cell cultures that the hormonal stimulation can be transmitted between the cells possessing gap junctional communication (Gilula et al., 1978; Lawrence et al., 1978).

In view of their occurrence in diverse organized tissues and importance in cell-to-cell communication, investigations have been aimed at understanding of their structure and correlation with functions, as well as the regulation of their operation.

The essential features of gap junctions appear to be similar throughout the animal kingdom. In thin sections, they appear as approximately 15-20 nm thick (McNutt and Weinstein, 1970) with a characteristic approximately 2 nm wide electron luscent "gap" in between the adjacent cells. By employing the colloidal lanthanum tracer, Revel and Karnovsky (1967) were able to demonstrate an "hexagonal lattice" in tangential sections of the gap junctions. With the advent of freeze- fracture technique (Steere, 1957; Branton, 1966), the presence of gap junctions can be readily registered. In the freeze-fracture replicas the gap junctions are frequently visualized as the quasi-crystalline lattice of intramembranous particles on the protoplasmic (P) fracture face and a complimentary lattice of pits on the ectoplasmic (E) fracture fact (see Chapter 4, Chalcroft and Bullivant, 1970; Bennett and Goodenough, 1978). [In the arthropod gap junctions, a reversal of the structure on the P and E faces is observed, Gilula, 1972]. These particles are named connexons (Goodenough, 1975).

These connexons are membrane-protein oligomers that span the phosopholipid bilayers of each of the adjacent membranes and enclose approximately 2 nm wide aqueous channel within (Goodenough, 1975). Caspar and coworkers (Caspar et al., 1977; Makowski et al., 1977), have investigated the structure of gap junctions by correlated X-ray diffraction and electron microscopic studies. Low angle X-ray diffraction

patterns from partially oriented gap junctions displayed a series of broad maxima on the meridian modulated by the effects of a quasi-regular stacking and partial orientation. After deconvoluting the meridional continuous intensity distribution for the factors mentioned above, electron density distribution perpendicular to the plane of junctions was calculated. Electron density distribution within the plane of gap junctions was calculated from the equatorial reflections with appropriate constraints provided by the electron microscope data. The three dimensional picture that emerged through such a study suggested a hexameric nature of the connexons. The electron density profile perpendicular to the plane of gap junctions (at a resolution of about 1 nm) revealed the existence of a pair of lipid bilayers with the polar groups separated by 4.2 nm across the bilayers and 4.5 nm across the gap (Makowski et al., 1977). The electron density in the region of low-density minimum in the center of the bilayers was considerably higher, than could be expected for pure lipid hydrocarbons. Therefore it was concluded that there is a significant protein content in this region (Makowski et al., 1977). The electron density projections within the plane of junctions failed to discern any subunit structure and connexons appeared to be as only circularly symmetric structures. These projections did not reveal much information about the structure of the connexons. Furthermore, the resolution in this study extended to a spacing of only about 2.5 nm.

A real breakthrough in our knowledge of the structure of gap junctions has come from the work of Unwin and Zampighi (1980) who have analyzed the low- dose electron micrographs of negatively stained

junctions by Fourier methods (DeRosier and Klug, 1968; Henderson and Unwin, 1975) and calculated a three dimensional map at 1.8 nm resolution. This map clearly revealed the connexon as a hexamer of subunits spanning the membrane and emerging from the cytoplasmic and extracellular faces of the membrane. The subunits are roughly rod-shaped, about 7.5 nm long and 2.5 nm in diameter These subunits are tilted with respect to the six-fold axis thus imparting the whole assembly a left-handed character. The central opening of the channel, enclosed within the subunits, is about 2 nm wide in the extracellular region of the membrane (where it is occupied by the hydrophilic negative stain) and narrows within the membrane where it is not resolved. Of greater significance, was the finding of a second form of gap junctions produced after extensive dialysis. This form of gap junctions has connexons in a different configuration presumably reflecting the channel in a 'closed' state. The second form conceivably resulted from a correlated radial and tangential displacement of subunits about the six-fold axis of symmetry passing through the center of the connexon. Marked radial displacement was postulated to occur near the cytoplasmic end where the central opening surrounded by the subunits disappeared as a consequence of the transition. On the cytoplasmic side, this radial displacement was of the order of 0.6 nm. Also as a result of this transition, from 'open' to 'closed' state, the mean inclination of the subunits relative to the six-fold axis was reduced from 14° to 9°. Thus Unwin and Zampighi's model for the first time provided a mechanism for the regulation of channel permeability emphasizing a small radial and tangential movement of subunits as the key feature of regulation. However,

the existence of a continuous aqueous channel throughout the connexon could not be resolved even in this study.

It is evident from the above that only scanty information is available on the structure of gap junctions. Structural studies thus far have been restricted to low-resolutions (extending up to approximately 1-8 nm) on account of considerable short range disorder (Caspar et al., 1977) and rather small sizes of crystalline domains (Unwin and Zampighi, 1980) in the available gap junction preparations. If well-extended two-dimensional hexagonal crystals of connexons can be obtained, their high resolution structure should be amenable to the classic low-dose, three-dimensional Fourier transform electron imaging and diffraction methods (Unwin and Henderson, 1975; Henderson and Unwin, 1975) that were employed so successfully in the determination of the structure of the purple membrane of Halobacterium halobium. A solution of the structure of gap junctions at high resolution would be of paramount importance in providing an insight into the functioning of these communicating channels, which are probably the largest known channels in eukaryotes (Evans, 1980). Understandably, considerable effort must be devoted to working out isolation methodologies that yield better two-dimensional crystals of gap junctions. When such gap junctions become available, important advances could come about over the existing limit on the attainable resolution and molecular details of these communicating channels be revealed.

There is also no agreement over the number and molecular weight(s) of constituent polypeptide(s) that make up the gap junctions (Goodenough and Stoeckenius, 1972; Goodenough, 1974; Duguid and Revel,

1975; Ehrhart and Chaveau, 1977; Hertzberg and Gilula, 1979; Henderson et al., 1979; Gilula, 1980). In many of these preparations collagenase and hyaluronidase (both having some non-specific protease activity) were frequently utilized to reduce the contamination of final gap junction preparations by collagen and amporphous proteins (Goodenough and Stoeckenius, 1972; Goodenough, 1976; Duguid and Revel, 1975; Caspar et al., 1977). Such a treatment could cause the proteolysis of the isolated gap junction fractions and consequently markedly alter the polypeptide composition (Duguid and Revel, 1975). Even after the enzymatic treatment was substituted by exposure to 1-6 M Urea to facilitate the isolation of morphologically enriched gap junctions (Hertzberg and Gilula, 1979; Henderson et al., 1979), the number of polypeptides and their molecular weights remain uncertain (Fallon and Goodenough 1981).

Investigations on the polypeptide composition of gap junctions are complicated by endogenous and exogenous proteolysis during the isolation and a marked propensity of the gap junctional polypeptides to aggregate in the presence of sodium dodecyl sulphate (SDS) (Henderson et al., 1979; Hertzberg and Gilula, 1979; Finbow et al., 1980; Nicholson et al., 1982). In spite of possible proteolysis, it appears that a predominant component in the liver gap junctions is a polypeptide of 25-27,000 daltons but the number of additional polypeptide(s) is in dispute (Fallon and Goodenough, 1981). It is of importance to establish the polypeptide composition of gap junctions and it is to this end that different isolation methodologies should be devised (which minimize both the endogenous and exogenous proteolysis).

Furthermore, it has been claimed that the currently available isolation procedures uncouple the gap junctions and induce the connexons to pack closely in two-dimensional hexagonal arrays (Perracchia, 1980). Therefore, in order to study the structural dynamics of these channels there is a need to develop methods to preserve their in situ structure.

The purpose of the present project is thus twofold: Firstly, to develop a method to isolate gap junctions (which could be suitable for high resolution structural studies) and characterize their polypeptide composition. Secondly, to gain an insight into the structure of these communicating channels in situ. I have carried out such investigations on the gap junctions of the mouse liver. Briefly a method has been developed to isolate gap junctions which employs a new solubilization protocol (for solubilizing the non-junctional plasma membranes) and eliminates the use of enzymatic treatments or exposure to denaturing action of urea. The hexameric subunit structure of the connexons in situ has been confirmed by employing rapid freezing and rotatory shadowing techniques in conjunction with Markham's rotational filtering method (Markham et al., 1963) for contrast enhancement. Also, a contraction of the lattice of connexons induced upon fixation with glutaraldehyde in the structure of gap junctions (uncoupling of gap junctions) has been elaborated.

2. HISTORICAL PERSPECTIVE: FROM SCHLIEDEN'S CELL THEORY TO CELL TO CELL COMMUNICATING CHANNELS: LOW RESISTANCE CHANNELS

The concept of cell as implicit in Schlieden's cell theory emphasized their role as "circumscribed, self contained unit beings" and attributed to a wall-like structure (to be later described as the plasma membrane by Nageli in 1855) a function of merely surrounding the cells and isolating them from the rest of the tissue (Schlieden, 1838). The function ascribed to the plasma membrane was that of a protective barrier which excluded the possibility of any exchange of material with the extracellular medium or the neighbouring cells.

This tenet was to survive unscathed until the last decade of 19th century when the highly active and specialized transport functions of the plasma membrane became known. However this necessitated only a small modification in the theory as the diffusion barrier for small inorganic ions had to be relaxed. Early workers who studied the transport phenomena (Overton, 1899; Gryns, 1896; Hedin, 1897) underlined the cruicial role of the oil-water partition coefficient of a molecule (corresponding to its lipid solubility) in determining how quickly it penetrated across the plasma membranes into the cells. Since then this conclusion has been greatly amplified and refined and has emerged as an important aspect of membrane behavior (Jacobs, 1935; Collander, 1937; Dawson and Danielli, 1943). At about the same time the existence of hydrophilic channels in the membranes was invoked and the surface membrane was pictured to harbour "sieve" like areas in

addition to the "lipoidic" areas (which were constituted predominantly of fatty acids) (Jacobs 1924; Hober, 1936; Collander, 1937). However, the idea of the existence of an incomplete diffusion barrier at the sites of cell-contact, in the cells of most organized tissue, is of relatively recent origin. Indications to this effect came initially from the work by Weidmann (1952) who had observed that in the cardiac muscle, a voltage change in one cell induced a corresponding voltage change in the neighbouring cell. A few years later Furshpan and Potter (1959) clearly established the existence of electrical coupling via a low-resistance pathway between the excitable cells in the crayfish nervous system. This elegant work marked the discovery of electrical synapse and was soon followed by the reports of electrical communication. However, all these accounts of intercellular electrical coupling were reported only in the cases of excitable cells where this might be considered as an adaptive feature of the membranes devoted to electrical mode of signal transmission. Moreover, electrical intercellular transmission could be easily attributed to the passage of small ions through the membrane channels not very different from those known to exist in the plasma membranes. Therefore, the discovery by Furshpan and Potter (1959) although epoch-making in its novelty, did not as yet spell any challenge to the cell theory's principal tenet of cell individuality. However, the discovery by Loewenstein and Kanno (1963, 1964) in the salivary glands of Chironomus and Kuffler and Potter (1964) in the glial cells of leech, of the existence of electrical coupling in nonexcitable tissues delivered a severe blow to the

cell-individuality principle. Moreover, Loewenstein and Kanno, (1964) also demonstrated that the size of the permeant molecule that could pass through cell junctions (flourescein, M.W. 330), was considerably greater from that of the organic ions that were known to be responsible for the transfer of electrical signals in nerve and muscle. Subsequent work revealed that a number of other small hydrophilic molecules of M.W. between 300-1000 daltons could also pass through these junctions (Kanno and Loewenstein, 1966; Potter et al., 1967). It became apparent that these molecules could not pass through the types of channels that were known at that time. Therefore it was proposed that these molecules actually passed through specialized junctional pathways comprised of leakproof, relatively large hydrophilic cell-to-cell channels, localized at the sites of cell-to-cell contacts (Loewenstein, 1966). Since then, the notion of cell individuality, which comprised the basic tenet of Schlieden's cell theory, has undergone revision. Cells in most organized tissues can no longer be considered as independent from each other especially in view of the restricted equilibration of the cytoplasmic constituents that can be facilitated and controlled by these intercellular communicating hydrophilic channels. Incorporated within these channels is also the capacity to allow the transfer or exchange of small metabolites which may be of relevence to developmental biologists (Crick, 1970, Wolbert, 1981, Gierer, 1981). Such permeable junctions have been identified throughout the phylogenetic scale, from sponges to man (Evans, 1980).

2.1 Ionic Coupling

A demonstration of the junctional permeability for intercellular transfer of small ions can be achieved by measuring electrical resistances across the boundries between continguous cells. The electrical coupling through low-resistance cell-to-cell channels is usually described as the capacity for passive (electrotonic) movement of transient electric potential from a cell to the neighbouring one cell (Socolar and Loewenstein, 1979) usually with very little voltage attenuation. The presence of electrical coupling can be displayed by transmitting pulses of electric (ionic) current, with the help of an intracellular microelectrode, between the interior of one cell and the external medium, and monitoring the consequent steady state transients of membrane potential with the help of another pair of microelectrodes in this cell and its nearest next neighbour cell (Socolar and Loewenstein, 1979). In the presence of electrical coupling the membrane potential of the nearest next neighbour cell would change. The ratio between the steady state rises of potentials between these two cells is the coupling ratio or coupling coefficient (Furshpan and Potter, 1959). [The electrical coupling is quite sensitive upon cell damage, or in the presence of certain chemicals which may have some harmful effects.]

The presence of low-resistance cell to cell (junctional) pathways in excitable tissues can be appreciated by the consideration that these pathways would facilitate rapid propagation of impulses of electrical nature, between the cells. The significance of the

existence of electrotonic synapses (electrotonic junctions) in the nervous system may lie in the evident temporal gains over the chemical synapses, owing to the rapid electrotonic transmission of electrical impulses which is well suited for quick responses (Bennett, 1977). Synchronization of the cardiac muscle cells into a functional syncytium is brought about by the rapid cell to cell spread of action potentials through these junctional channels (Weidman, 1952). The contrast between the properties of these low-resistance channels and chemical post synaptic channels becomes evident upon a consideration of the inherent lack of charge discrimination in the former. Both small cations ($^{42}K^+$, $^{86}Rb^+$, CO^{2+}, $^{22}Na^+$), and anions ($^{36}Cl^-$, $^{125}I^-$, $^{35}SO_4^-$) have been demonstrated to cross these channels (Reviewed by Peracchia, 1980).

By exploiting the simple geometrical shapes of the cells in cultured Novikoff hepatoma cells, Sheridan et al. (1978) have reported rather reliable values for the specific resistance of the junctional membranes. Specific junctional resistance has been measured to be $0.3 - 1.2 \times 10^{-2}$ $/cm^2$. The rather 'low' resistance of the intercellular pathway becomes evident when compared with the specific resistance of the non-junctional membrane which is estimated to be $1000\text{-}2600^2$ $/cm2$ (Trautwein et al., 1956, Van der Kloot and Dane, 1964). Also when compared with other excitable channels e.g. Na^+ channels (2.4×10^{11} , Conti et al., 1975) and K^+ channels (8×10^{10} , Conti et al., 1975), the resistance of intercellular channels appears to be quite low.

2.2 Dye-Coupling

Gap junctional pathways have also been demonstrated to be permeable to injected fluorescent dyes of low molecular weight (Socolar and Loewenstein, 1979). The first such probe to be employed was a 330 dalton, flourescent anion of flourescein (Loewenstein and Kanno, 1964). However, later on it became apparent that flourescein anion was not only transferred through the junctional route, but through the nonjunctional membranes as well. In order to remedy this problem, Procion yellow M4RS was introduced as a flourescent tracer dye (Payton et al., 1969) with a rather weak flourescence and more affinity for binding to cytoplasmic components which retarded its intracellular diffusion (Stretton and Kravitz, 1973). This was also demonstrated to permeate through the non-junctional membranes in some cells and have toxic properties for others. Recently, 6- carboxyflourescein (Socolar and Loewenstein, 1979) has been introduced as the flourescent tracer. A number of other dyes [and radioactive tracers] have also been shown to diffuse across the cells through the junctional pathways.

By conjugating a variety of natural and synthetic peptides with flourescent dyes, systematic investigations of molecular size limit for junctional permeation have been undertaken by Loewenstein's group (Simpson et al., 1977, Loewenstein, 1981). The channels in the mammalian cells appear to have more limited channel bore in comparison to those of insect cell cultures. Mammalian channels also display greater charge discrmination to the negatively charged molecules of a series, a feature which appears to be less prominent in the insect channels (Loewenstein, 1981). The extent of charge discrmination appears to be selective enough to distinguish between the charges on

the peptide backbones of fluorescent peptide molecules and furthermore to detect the second order effects of charge delocalization on the fluorophore (Loewenstein, 1981). This is supported by a marked preference for a lissamine rhodamine B (LRB) - labeled molecule over fluorescein isothiocynate (FITC) - labeled one. There is one delocalized positive charge on LRB and an almost equal negative delocalized charge on FITC (Flagg-Newton et al., 1979). Very little is known about the charged permeants. The channel diameter appears to be at least 1.6 nm, a figure which is compatible with the smallest dimensions of the largest permeant molecules. Upon probing with an uncharged (neutral) set of glycopeptides, the channel diameter of the insect channels was measured to be approximately 2-3 nm and of the mammalian cells approximately 1.6-2 nm, (Schwarzmann et al., 1981).

2.3 Metabolic Coupling

Subak-Sharpe et al. (1966, 1969) were the first to describe contact-dependent transfer of radiolabeled metabolites through specialized permeable junctions. These authors, while working on tissue cultures of hamster fibroblasts, discovered that certain mutant cells were devoid of the enzyme hypoxanthine-guanine phosphoribosyl transferase (HGPRT), and thus were incapable of incorporating a nucleic acid precursor into their nucleic acids. However, these could become capable of incorporation, if grown with the wild type cells in a medium containing [^{3}H] hypoxanthine. Only those mutant cells manifested the incorporation which are either in direct contact with the wild type

cells or through other mutant cells. That the presence of such a contact was crucial for the incorporation of hypoxanthine in the mutant cell was further evidenced by the cessation of incorporation upon physical separation (Hooper and Subak-Sharpe, 1981). It appears that in all these cases, the molecular species which was transferred to the recipient cell was probably a nucleotide and not a macromolecular species like RNA as has been claimed by Kolodny (1972).

2.4 Gap Junctions Mediate Ionic and Metabolic Coupling

What is the evidence for gap junctions as the structural pathways for mediating both ionic coupling and metabolic coupling concomitantly? Employing the co-culture combinations of communication competent, and communication-deficient cells, it was demonstrated that in the co-cultures of communication-competent cell types, both ionic and metabolic couplings can occur simultaneously (Gilula et al., 1972). In the co-cultures of communication competent and deficient cells, as expected, ionic and metabolic coupling were absent (Gilula et al., 1972; Azarina et al., 1972). Since the same contact was used by both of these phenomena and gap junctions were observed at the sites of cell to cell contact, it seems reasonable to assume that most likely (but not exclusively) gap junctions mediated both the ionic as well as metabolic coupling. This conclusion was further strengthened by the absence of gap junctions noticed between cells that were incapable to communicate.

The role of cAMP as a mediator in the intercellular communication has been demonstrated by Lawrence et al. (1978). The intercellular communication was investigated in the heterologous co-cultures of

rat ovarian granulosa cells and mouse myocardial cells. They documented the existence of electrical coupling and the establishment of gap junctions between the heterologous cells. Furthermore, ^{3}H-uridine or ^{3}H-adenine was exchanged between the cells. When one cell type was prelabelled, the presence of isotope in the heterologous cell was confirmed by autoradiography. Both of these cell types have characteristic hormonal responses, the myocardial cells respond to noradrenaline whereas the ovarian granulosa cells respond to follicle stimulating hormone (FSH). Both of these hormones elicit their effects by mediation through cAMP. Therefore, the hormonal stimulation of one cell type will elicit the stimulation of the coupled cell of the other type, in the heterologous co-cultures. This was experimentally verified. Noradrenaline-induced stimulation of myocardial cells results in production of plasminogen activator, a response characteristic of granulosa cells upon stimulation by FSH. Likewise, FSH induced stimulation of granulosa cells causes an increase in the beat frequency of the myocardial cells. Since cAMP mediates the responses elicited by both of these hormones it is reasonable to assume that this molecule is most likely involved in the mediation of intercellular communication between the heterologous cell types.

2.5 The Regulation of Junctional Permeability

The porosity of gap junctional channels appears to be modulated by a variety of factors that alter the intracellular homeostasis which in turn reset the degree of intercellular coupling. The coupling is also liable to fall markedly and may cease to a complete halt in the face of damage or injury to the one or more of the involved cells. Uncoupling has also been induced by raising the intracellular

concentration of free Ca^{2+} (Loewenstein, 1966). Loewenstein has proposed that the concentration of free cytoplasmic Ca^{2+} concentration is low, and when Ca^{2+} concentration is high the porosity would decline. However, recently intracellular pH has been claimed to be the modulator of the channel permeability (Turin and Warner, 1977). In some cases voltage dependent junctional permeability has also been described by Bennett's group (Bennett et al., 1981). The coupling through these channels appears to be a passive process with no energy demands with a rate of transfer of the same order of magnitude as passive cytoplasmic diffusion (Gilula, 1980).

3. ISOLATION AND STRUCTURAL CHARACTERIZATION OF GAP JUNCTIONS

3.1 Introduction

It must be emphasized at the outset, that no endogenous activity as yet has been detected in the gap junctions and morphological criterion is the only major assay for evaluating the purity of the subcellular fractions enriched in gap junctions. One of the earliest methods employed for the isolation of gap junctions was based on the premise that gap junctions seem resistant to certain detergent treatment that disrupts the non-junctional plasma membranes (Benedetti and Emmelot, 1968). On this basis, Benedetti and Emmelot (1968) obtained sub-cellular fractions enriched in gap junctions by simply treating the rat-liver plasma membranes with deoxycholate which solubilizes the non-junctional plasma membranes. But subsequently, deoxycholate treatment was demonstrated to cause irreversible structural changes in gap junctions, leading to a collapse of the gap region (Goodenough and Revel, 1970).

Goodenough and Stoeckenius (1972) and Evans and Gurd (1972) arrived at the choice of n-lauryl (dodecyl) sarcosine to enrich the plasma membrane fractions for gap junctions. As a conseqence of this detergent treatment of plasma membranes, a large amount of partially solubilized amorphous debris was produced together with the contaminating collagen fibres and uricase crystals. Therefore, these isolation procedures involved treatment of plasma membranes with hyaluronidase and collagenase to reduce the contamination of the final preparations. Subsequent centrifugation in a sucrose density gradient, yielded

morphologically pure gap junctions. After the enzymatic treatments, although the overall morphological features were still conserved, the constituent proteins were found to be partially degraded (Duguid and Revel, 1975), and hence there was no accord amongst the workers over the number and molecular weights of constituent polypeptides (Goodenough, 1974; Culvenor and Evans, 1977; Ehrhart and Chaveau, 1977).

In 1979, three methods were reported in which proteolysis was minimized by eliminating the enzymatic treatment. Instead, the purification in two of these methods was facilitated by exposure to 1-6 M urea. One of these methods employed Triton X 100 (Henderson et al., 1979) whereas the other employed n-lauryl sarcosine (Hertzberg and Gilula, 1979). Both of these detergents solubilize the non-junctional plasma membranes (see above). The third method introduced by Zampighi and Unwin (1979) utilized deoxycholate and Lubrol-WX. However, it seems that the problem of proteolysis was not completely resolved. This together with the pronounced aggregation of gap junctional polypeptides in SDS (Henderson et al., 1979) resulted in an apparent heterogeneity in the reported polypeptide profiles. The constituent polypeptide(s) of the gap junctions (named connexin by Goodenough, 1974) are intrinsic (integral) membrane proteins based upon a value of 0.322 for the Barrantes (1975) discriminant function Z and freeze-fracture data (Bennett and Goodenough, 1978).

A detailed consideration of the specific interactions of the integral membrane proteins with phospholipid bilayers provides with a rationale for the choice of an appropriate amphiphile (detergent) to

solubilize and isolate such proteins in their native states (see Appendix 'A').

3.2 Materials and Methods

3.2.1 Experimental system: mouse liver

For the isolation and characterization of gap junctions, mouse liver was an appropriate choice. Even though mouse has the evident disadvantage of providing less liver per animal, this is more than compensated for by the following:

a) greater yield of plasma membranes per gram of liver;

b) ease of homogenization due to relatively small amounts of connective tissue;

c) low levels of collagen contamination of the final preparations;

d) large size of the murine hepatocyte gap junctions.

3.2.2 Isolation Procedure for Gap Junctions

Initially when the isolation work was undertaken, the gap junctions were isolated by the method of Goodenough and Stoeckenius (1972). Then for some time Hertzberg and Gilula's method was employed (Hertzberg and Gilula, 1979). Attempts were also made to adopt the method proposed by Henderson et al., (1979) based upon the use of Triton X100. However, these methods had to be abandoned because of the low-yields and inconsistent purity in my hands. Therefore, attempts were made to develop an isolation protocol by using a wide variety of detergents, by essentially trial and error method.

Figure 1

A flow-chart for the isolation of plasma membranes from the mouse liver.

WHOLE LIVERS

Dounce homogenization
4 livers/40ml homogenization medium

HOMOGENATE

Isolation medium
filter (34+2 layers cheese and nylon cloth)

FILTRATE

centrifugation, GSA rotor
8000 rpm , 30 MIN

PELLET

WASH with isolation med.
centrifuge as before

PELLET

WASH and centrifuge as before

PELLET

WASH and centrifuge as before

PELLET

isolation medium
67% w/w sucrose in isol. med.

SUCROSE in isol. med.

37% w/w
41% w/w
45% w/w

SAMPLE

centrifugation
SW-28 rotor
26000 rpm
90 MIN

37-41% w/w interface is enriched in plasma membranes

THE ISOLATION OF PLASMA MEMBRANES

An isolation procedure for gap junctions has been developed which involves solubilization of plasma membranes by an anionic detergent n-dodecanoyl sarcosine in combination with non-ionic polyoxyethylene alcohol detergents (Brig 35, Brig 58) and a non-ionic polyoxyethylene ether (W-1) detergent. Subsequent centrifugation is performed in a sucrose gradient containing 0.1 mM 1-O-n octyl-β-(D) glucopyranoside. It is emphasized that some of these detergents have not been previously used in the solubilization of the plasma membranes. The isolation protocol is outlined below in detail. All isolation procedures were carried out at 4°C unless noted otherwise.

3.2.2.1 Isolation of Plasma Membranes

In some initial experiments, plasma membranes were prepared by a modification of Neville's method (Neville 1960). However, in view of the lower yields of plasma membranes and hence of gap junctions this method was abandoned. Inclusions of Ca^{2+} (Ray, 1970) and sodium borate (Dorling and LePage, 1973) in the homogenizing medium have been claimed to improve the yield of plasma membranes. However, my attempts to incorporate these modifications in the original Neville's (1960) method always resulted in excessively contaminated and aggregated membrane preparations. Attempts were also made to employ the aqueous two-phase polymer system for the isolation of plasma membranes, but it could not be used efficiently for bulk purposes (Lesko et al., 1973). There were a total of about 80 attempts to isolate the plasma membrances by various methods. The method described below has been employed successfully for more than 15 times. Protein concentrations were determined by Lowry's method (Lowry et al., 1951).

Plasma membranes were isolated (see Fig. 1) by a modification of the method of Fallon and Goodenough (1981)

Homogenization medium

1.5 mM EGTA
1 mM $NaHCO_3$
2 mM Phenylmethylsulfonylfluoride (PMSF)
1 mM Parachloromercuribenzoate (PCMB)
1 mM Dithiothreitol (DTT)
pH 8.5,

Isolation medium

1 mM EGTA
1 mM $NaHCO_3$
1 mM PMSF
1 mM PCMB
1 mM DTT
pH 8.0

40 white mice (30-40 days old) were sacrificed by cervical dislocation. Livers were immediately dissected out, and homogenized in a 40-ml dounce homogenizer (Belco, U.S.A.) with a loose type "B" pestle, in approximately 40 ml of homogenization medium per four livers, by 8-10 strokes. The homogenate was diluted to 2000 ml with the isolation medium stirred and allowed to stand for 10 minutes. Then it was filtered slowly through 35 layers of cheesecloth (Curity, grade 50, The Kendall Comp.) followed by filtration through 2 layers of 63 mesh nylon cloth (precipitated material at the bottom was not filtered and discarded). The filtered homogenate was centrifuged in a GSA rotor, 8000 rpm for 30 minutes (3×10^5 g minute). The supernatant was aspired off and discarded. The pellets were resuspended by vigorous shaking in 4000 ml of isolation medium and centrifuged at 8000 rpm in a GSA rotor for 30 minutes. The resulting supernatant was again removed by

Figure 2

A flow-chart describing the solubilization of the non-junctional plasma membranes and the isolation of the gap junctions.

PLASMA MEMBRANES

1) SOLUBILIZATION MEDIUM (1mM EGTA, 2mM $NaHCO_3$, 1mM DTT and 1mM PMSF, pH 9) at room temperature
2) 1%(w/v) n-dodecanoyl sarcosine in solubization medium, room temp., 5 MIN
3) 3100 rpm, SS-34 rotor, 10 MIN

N-DODECANOYL SARCOSINE SUPERNATANT

1) 0.5% (w/v) BRIJ 35 in solubilization medium, room temp., 5 MIN
2) 17,000 rpm, SS-34 rotor, 15 MIN

BRIJ-35 AND N-DODECANOYL SARCOSINE PELLET

1) solubilization medium at room temp.
2) 0.2%(w/v) BRIJ 58 and polyoxyethylene ether W-1(0.25% w/w) in solubilization medium at room temperature

POLYOXYETHYLENE ETHER W-1 AND BRIJ-58 TREATMENT

CENTRIFUGATION

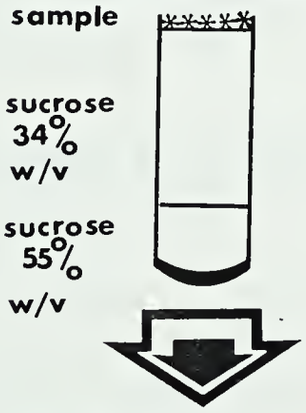

SUCROSE GRADIENTS IN 0.1mM 1-O-n-octyl-β-D-glucopyranoside in the solubilization medium at 4-8°C.

30,000 rpm, SW-40 rotor, 120 MIN at 4°C

34–55 % w/v interface is enriched in gap junctions

THE ISOLATION OF GAP JUNCTIONS FROM PLASMA MEMBRANES

aspiration and discarded. Whereas the pellets were resuspended by vigorous agitation through no. 13 needle in 4000 ml of isolation medium and centrifuged again as before. The resulting pellets were suspended in approximately 200 ml of isolation medium this time (supernatant was again discarded) and centrifuged as before. The supernatant was carefully aspired off leaving the underlying pellet undisturbed. The pellet was dislodged and suspended in the minimum possible volume of isolation medium, by vigorously drawing up and down through a no. 13 needle. The volume was accurately measured. To this with, constant stirring, slowly drop by drop 2 times its volume of 67% (w/w) sucrose in isolation medium was added. This suspension was underlaid in SW28 rotor tubes (Beckman) and overlaid with 45% (w/w), 41% (w/w) and 37% (w/w) sucrose solutions prepared in the isolation medium. These step gradients were centrifuged at 26,000 rpm for 75 minutes (7.5×10^6 g per minute). The plasma membranes gathered as a visible band at 37% (w/w) - 41% (w/w) interface, were harvested by a pasteur pipette (1.5 - 2 mg plasma membranes/gm liver).

3.2.2.2 Solubilization of Plasma Membranes and Isolation of Gap Junctions (Fig. 2)

Plasma membranes were suspended in approximately 1500 ml of isolation medium and centrifuged in a GSA rotor at 10,000 rpm for 30 minutes (4.9×10^5 g per minute). Resulting pellets were resuspended in approximately 500 ml of isolation medium and spun as before. These pellets were suspended in approximately 40 ml of 1 mM EGTA, 2 mM $NaHCO_3$, 2 mM DTT and 2 mM PMSF buffer, pH 9.0 (henceforth called as solubilization medium), at room temperature.

3.2.2.2.1 Treatment with detergents

3.2.2.2.1.1 Treatment with n-dodecanoyl sarcosine and Brij 35

To this suspension approximately 40 ml of n-dodecanoyl sarcosine was added (1% w/v, in solubilization medium, pH 9.0) slowly drop by drop with constant stirring provided by a magnetic stirrer at room tempterature. After 5 minutes at room temperature, it was centrifuged at 4-5°C in a SS-34 rotor (Sorvall), at 3100 rpm for 10 minutes (10^4 g min.). The supernatant was kept at room temperature, and small pellets (which were unevenly distributed at the bottom and had mostly collagen), were discarded. 10 ml of Brij 35 (0.5% w/v in 1 mM EGTA 2 mM $NaHCO_3$, 1 mM DTT and 1 mM PMSF, pH 9.0, buffer) was slowly added to the supernatant, followed by an incubation at room temperature for 5 minutes and centrifugation in a SS-34 rotor at 17000 rpm for 15 min. at 4-5°C. The supernatant was aspired out and discarded.

3.2.2.2.1.2 Treatment with Brij 58 and polyoxyethylene ether W-1

The pellets were suspended in 2 ml of solubilization medium. The suspension was accomplished by employing a hand driven **D**ou**n**ce homogenizer with a type 'B' pestle (8-10 strokes). To this 1 ml of 0.2% w/v Brij 58 and 1 ml of 0.25% w/v of polyoxyethylene ether (W-1) in the solubilization buffer was added at 4°C and very well mixed.

3.2.2.2.2 Density gradient centrifugation

This was loaded on the top of two-step gradients prepared in four SW-40 (Beckman) rotor tubes with approximately 5 ml of 50% w/v and approximately 7 ml of 33.81% w/v sucrose in solubilization buffer.

Incorporation of 0.1 mM 1-O-n-octyl-β-D-glucopyranoside (n-octyl glucoside) facilitated better separation of gap junction in the gradient. In some experiments, 0.1 mM sodium taurodeoxycholate was used in place of n-octylglucoside in the sucrose gradients with almost comparable results. These gradients were centrifuged in SW 40 rotor at 30,000 rpm for 2 hrs. at 8°C. The gap junctions usually gathered at the 33.81-50% w/v sucrose interface, could be visually observed as a band and harvested with a syringe. Washings were performed with the isolation medium (SW-40 rotor, 30,000 rpm, 45 min.). Finally, these gap junctions were suspended in 100-200 ml of the isolation medium.

Yield: 100-400μg protein/40 mice.

3.2.3 Electron Microscopy

Negative Staining: For negative staining a small aliquot of a gap junctional fraction (1 mg/ml) was deposited on freshly prepared carbon-coated grids and negatively stained with 1% (w/v) aqueous uranyl acetate (Finch, 1975). The grids were scanned in a Phillips EM400 (operated with a liquid N_2 cooled anticontamination device) at low magnification to locate the well-stained areas. Electron micrographs of stained gap junctions were usually taken at a magnification of x 36000 - 46000.

3.2.4 Optical Diffraction

Optical diffraction experiments were performed on a Polaron electron micrograph optical-diffractometer (model M802). This instrument employs a 2 milliwatt helium-neon laser as the source of coherent

light (λ = 632.8 nm). Electron micrographs of negatively stained gap junctions, suitably masked to expose only the particular areas of interest, were used as objects in the optical diffraction experiments. Optical diffractograms were recorded on 5" x 4" Polaroid (black and white) positive-negative plates.

3.2.5 X-ray Diffraction

To prepare the oriented specimen for X-ray diffraction, the isolated gap junctions were centrifuged at 260,000 xg for approximately 12 hrs. in a hemihyperboloid BEEM polyethylene capsule mounted on an adaptor that fits snugly at the bottom of a Beckman SW-60 rotor tube, at 4°C. After the appropriate trimming of the capsule to expose the specimen, it was mounted in a wet cell (kept at 4°C) with the incident X-ray beam parallel to the plane of the gap junctions. The X-rays were generated on a Elliot GX13 rotating anode X-ray generator with a 0.1 x 2.0 mm focal spot source and a double mirror Franks type camera. The diffraction patterns were recorded on a CEA reflex film and developed in full strength Kodak D19 for 6 min. A Perkin-Elmer microdensitometer was used to digitize the film and optical densities lying along the arcs and within a 30° sector centered on the equator were averaged employing a program written by D. Austen (These experiments were performed with the help of Prof. P.N.T. Unwin and P.Ennis at Stanford University).

3.2.6 SDS-Polyacrylamide Gel Electrophoresis

3.2.6.1 Apparatus

Electrophoresis in the presence of SDS, in polyacrylamide gels was carried out using the discontinuous buffer system of Laemmli (1970) employing vertical slab gels. A Protean dual slab cell (Bio-Rad Laboratories, Richmond, Calif.) with 160 x 120 mm glass plates and 1.5 mm thick spacer was used for making vertical slab gels containing 10% (w/v) acrylamide in the separating gels and 5% (w/v) acrylamide in the stacking gel. SDS-PAGE was run on the same apparatus. A teflon comb (25 mm teeth) was used to provide 15 sample wells in which the samples could be loaded.

3.2.6.2 Preparation of Gels

3.2.6.2.1 Separating Gels

10% (w/v) acrylamide gels were used throughout. 35 ml of the gel mixture could be prepared by adding the following to a conical flask:

8.75 ml of separating buffer (1.5m tris-HCl, 0.008 M EDTA, pH 8.9),

11.5 ml of 30% (w/v) acrylamide (29.2% acrylamide and 0.8% bis-acrylamide),

0.35 ml of 10% (w/v) SDS,

0.035 ml of TEMED and

10.9 ml of water.

Addition of 3.5 ml of 0.3% (w/v) ammonium persulphate (freshly prepared and deaerated for about 10 minutes) initiates the polymerization

reaction. The gel mixture was quickly transferred into the glass sandwich, with the help of syringe attached to a narrow plastic tube, taking care not to leave the air bubbles trapped inside. The glass sandwich filled up to approximately 20 mm from the top with the polymerizing gel and the gel top overlaid with about 2 ml of distilled water. It took about 45 minutes for the gel to polymerize. Thereafter, the water and the residual unpolymerized material at the gel surface were washed off with the distilled water and the upper buffer chamber was replaced over the sandwich.

3.2.6.2.2. Stacking Gels

To prepare the stacking gel mixture (5% acrylamide, 0.1% SDS and 0.125 M Tris-HCl, pH 6.8), 2.5 ml of stacking buffer (0.5 M Tris-HCl, 0.008 M EDTA, pH 6.8), 1.7 ml of 30% (w/v) acrylamide, 0-1 ml of 10% (w/v) SDS, 0.01 ml of TEMED and 2.7 ml of water are added together followed by stirring and deaerating for about 10 minutes. After the addition of 3 ml of 0.3% (w/v) ammonium persulphate (prepared fresh and deaerated) to initiate polymerization, the gel mixture was quickly poured onto the separating gel surface, upto the lower end of the upper buffer chamber trough.

A teflon comb was immediately inserted into the stacking gel mixture to form the sample wells. After about 30-60 minutes for permitting the gel to polymerize, the comb was taken out and the gel surface thoroughly rinsed with water.

3.2.6.3 Sample Preparation

Samples for SDS-PAGE were prepared by solubilizing freshly isolated gap junctions with vigorous pipetting in SDS-sample buffer (10% w/v glycerol, 5% w/v 2-mercaptoethanol, 2% w/v SDS and 0.0625 M Tris-HCl, pH 6.8) at room temperature for about half an hour. Approximately 50-70 µl of samples (containing about 40-80 mg of protein) were delivered into the sample wells employing a Hamilton syringe.

3.2.6.4 Electrophoresis

Upper buffer chamber and lower buffer tank were filled with electrode buffer (0.025 M Tris base, 0.192 M glycine and 0.1% SDS). Subsequently, the upper buffer chamber along with the slab gel was replaced over the lower buffer tank containing enough electrode buffer to immerse the slab gel totally and thus provide efficient cooling. The gels were initially run at 20 mA until the dye front arrived at the stacking - separating gel interface. Then the current was stepped up to 30 mA until the dye front approached the bottom of gel. The electrophoresis was usually carried on for about 5 hours.

3.2.6.5 Staining Procedures

For detecting proteins in polyacrylamide gels, a silver staining procedure due to Wray et al. (1981) was followed. At the end of electrophoresis, the gel slabs were taken out of the electrophoresis cell, the spacers removed and the glass plates were taken apart by squirting water (between the gel and the plates) and exerting some pressure with the plastic comb. The gels were given a brief rinse with

water and subsequently immersed in 50% methanol overnight with 2 or 3 changes. The gels were stained in ammonical silver nitrate solution for 15 minutes with constant agitation throughout. This solution is prepared by adding 4 ml of 20% (w/v) silver nitrate solution dropwise with constant stirring into 21 ml of 0.36% sodium hydroxide + 1.4 ml of 14.8 M ammonium hydroxide. The final volume was made up to 100 ml with double distilled water. This solution must be used within 5 minutes of its preparation. The staining is followed by a wash in deionized water with gentle agitation for 5 minutes. The gels were washed again and immersed in the developer until the bands become visible. The developer was prepared by adding 0.5 ml of 38% formaldehyde to 5 ml of citric acid. The final volume was made up to be 1 litre with double distilled water. Only fresh solution was used. Usually the optimum band development took less than 10 minutes. Finally the gels were washed in water and immersed in either 50% (v/v) methanol or 45% (v/v) methanol + 10% (v/v) acetic acid to stop any further stain development.

3.2.6.6 Photography, and Drying of the Gels

Immediately after the staining, the gels were photographed by employing transmitted light, on a Kodak Panachromatic-X (ASA 32) film. The gels were dried under vacuum at 90-95°C.

3.3 Results

3.3.1 Isolation of Gap Junctions

A procedure detailed in Section 3.2.2 has been developed for the isolation of highly purified gap junction fraction from mouse liver

plasma membranes. This procedure avoids the use of exogenous proteases and urea that have been commonly included in protocols of isolation of gap junctions (Casper et al., 1977; Henderson et al., 1979; Hertzberg and Gilula, 1979). The bulk isolation of plasma membranes from mouse liver was based upon a modification of a procedure due to Fallon and Goodenough (1981). The plasma membranes were first treated with an anionic detergent, n-dodecanoyl sarcosine, in combination with a non-ionic polyoxyethylene alcohol detergent, Brij 35, to solubilize the non-junctional plasma membranes. The insoluble fraction was further solubilized with polyoxyethylene alcohol (Brij 58) and polyoxyethylene ether (W-1). Subsequent centrifugation in a sucrose step gradient in the presence of 0.1 mM 1-o-n-octyl-β-D-glucopyranoside (a non-ionic detergent) to facilitate the separation, yielded a highly enriched gap junction fraction. It is emphasized here that some of the detergents (n-dodecanoyl sarcosine, W-1, 1-o-n-octyl-β-glucopyranoside) employed in this isolation protocol have not been previously used for this purpose. The incorporation of 1 mm EGTA throughout the isolation protocol provides exceptionally high yields of gap juntions (200-400 ug protein/40 mice) as originally documented by Fallon and Goodenough (1981).

As stated above, in the absence of any biochemical assay, the morphological evaluation is the only criterion for assessing the purity of the isolated fractions.

Plate 1

Figure 3

Electron micrograph of a negatively stained preparation of isolated gap junctions. The gap junctions often lie flat on the grid in the form of plaques of various shapes and sizes, often reaching approximately 1μm on the edge. The hexagonally packed connexons are evident. (A magnified view is shown in Figure 7). The encircled area has been subjected to optical diffraction.


0.1μm

3.3.2 Structural Characterization

3.3.2.1 Electron imaging of negatively stained gap jucntions and optical diffraction

Electron microscopical examination of the negatively stained gap junction fractions provides a quick means of evaluating the purity of the preparations. Fig. 3 shows a typical preparation of gap junctions isolated by the new procedure. The gap junctions were in the form of plaques of various shapes and sizes with lateral dimensions as large as 1 um. They consisted of hexagonal arrays of connexons. Each annular connexon appeared to be well-defined with a electron-dense spot about 1.5 - 2.0 nm wide at the center. This spot is due to the accumulation of the negative stain at the six-fold axis that correponds to the putative hydrophilic channel. In order to ascertain the lattice constant representing center-to-center spacing of these gap-junctions more objectively, their electron micrographs were subjected to optical diffraction analysis. The resulting optical diffraction patterns (Fig. 4a) displayed reflections that could be indexed on a two-dimensional hexagonal lattice extending out to 2,0 reflection, in the normal high-dose electron micrographs. A few specimen diffracted out to the 3,0 reflection (Fig. 4b). The lattice constant appeared to be in the range of 7.6 - 8.4 nm presumably depending upon the degree of lipid solubilization by the detergents. The potential of these gap junctions for providing high-resolution structural information by low-dose electron imaging is yet to be explored.

Plate 2

Figure 4

a. The optical diffraction pattern corresponding to the area enclosed by the circular mask displayed in Figure 3. The diffraction pattern can be indexed on a hexagonal lattice of lattice constant approximately 8.2 nm, and extends to the 2,0 reflection. In a few cases (Fig. 4b) the diffraction pattern extends out to the 3,0 reflection.

For a hexagonal system:

$$a = b \neq c$$
$$\alpha = \beta = 90^{\circ}$$
$$\gamma = 120^{\circ}$$

The d_{hkl} spacing formula for the hexagonal system:

$$\frac{1}{d_{hkl}^2} = \frac{4(h^2 + hk + k^2)}{3a^2} + \frac{l^2}{c^2} \qquad \text{..... (a)}$$

Since in the case of gap junctions, the incident electron beam is parallel to the z axis, the zone axis of the diffraction pattern would be [001]. And hence **l** index for all the diffraction spots would become zero, thereby reducing the equation (a) to the following form:

$$\frac{1}{d_{hkl}^2} = \frac{4(h^2 + hk + k^2)}{3a^2} \qquad \text{..... (b)}$$

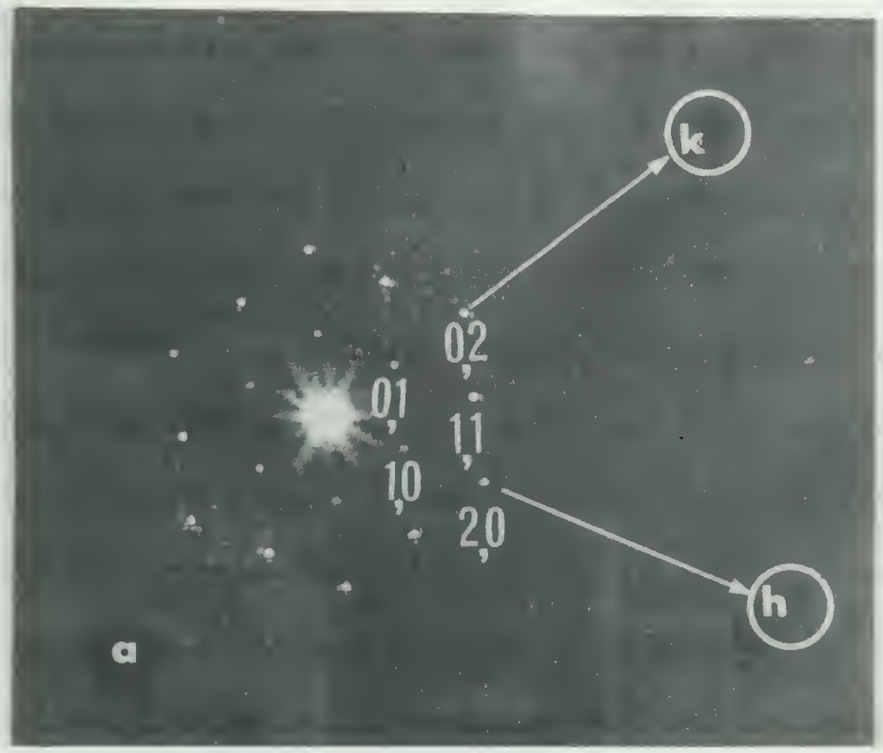
k
0,2
0,1
1,1
1,0
2,0
h
a

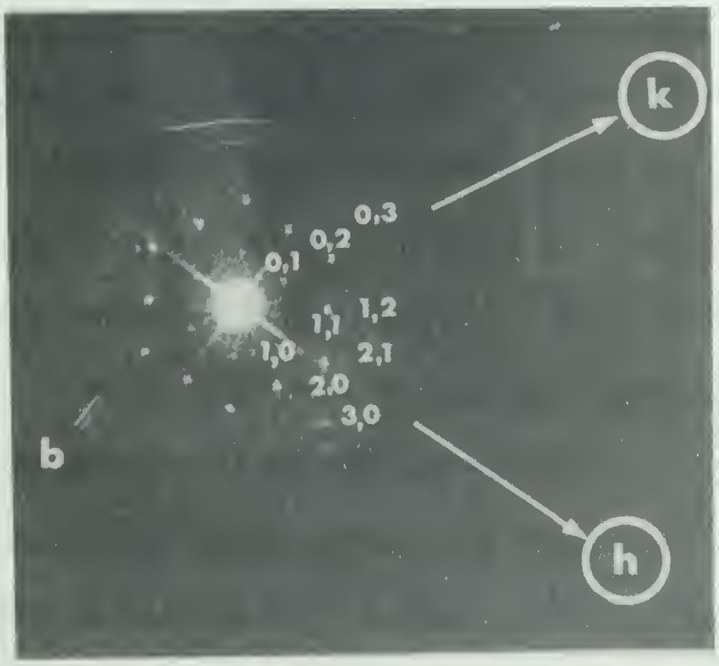
k
0,3
0,2
0,1
1,1
1,2
1,0
2,1
2,0
3,0
b
h

In some preparations gap junctions displayed a tendency to curve and even undergo partial vesicularization (Fig. 7). This phenomenon fortuitously offered the edge-on views of gap junctions in a direction nearly parallel to the plane of junctions, thereby providing the density variations along the 0,0 and 1,1 lattice lines. These images displayed the 2 nm characeristic "gap" between the apposed plasma membranes forming the gap junction, clearly delineated by the penetration of uranyl acetate into this region. The gap was traversed by periodically arranged particles surrounded by the electron dense stain. The tendency to curl up appears to be markedly pronounced with prolonged treatment with detergents which could be due to an extensive removal of lipids.

3.3.2.2 X-ray Diffraction on Partially Oriented Gap Junctions

When the plane of gap junctions in partially oriented pellets was nearly parallel to the incident x-ray beam, the x-ray diffraction pattern displayed a series of arcs along the equator and diffuse maxima along the meridian (Caspar et al., 1977; Makowski et al., 1977). The equatorial diffraction from the membrane corresponds to the projection of electron density along the unique axis(z). It is due to "sampling" of molecular transform by the reciprocal lattice (Hosemann and Bagchi, 1962; Guiner, 1963 and James 1965). The meridional diffraction is caused by the electron density distribution perpendicular to the plane of the gap junction. The crystalline packing of connexons within the plane of the gap junction gave rise to the arcs along the equator which could be indexed on the basis of a hexagonal

Plate 3

Figure 5

A low-angle X-ray diffraction pattern of partially oriented gap junctions. The X-ray beam was parallel to the plane of the junctions. The set of arcs centered on equator (1,0; 1,1; 2,0 and 2,1) corresponds to a hexagonal lattice of lattice constant approximately 8.2 nm. The equatorial diffraction is due to the electron density distribution (sampled on a hexagonal lattice) within the plane of the gap junction. Whereas the meridional diffraction is due to the electron density distribution perpendicular to the plane of the gap junction.

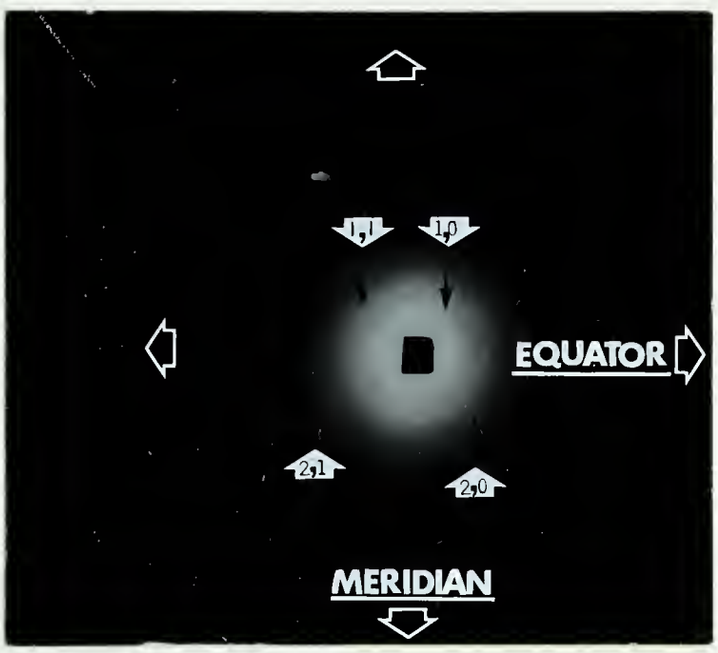
1,1
1,0
EQUATOR
2,1
2,0
MERIDIAN

Plate 4

Figure 6

A microdensitometer recording of the equator of the diffraction pattern displayed in Fig. 5. The arrows mark the expected positions of the reflections from a hexagonal lattice with the lattice constant of 8.178 nm. The position of 2,1 reflection departs slightly from that calculated and is shifted towards higher radius.

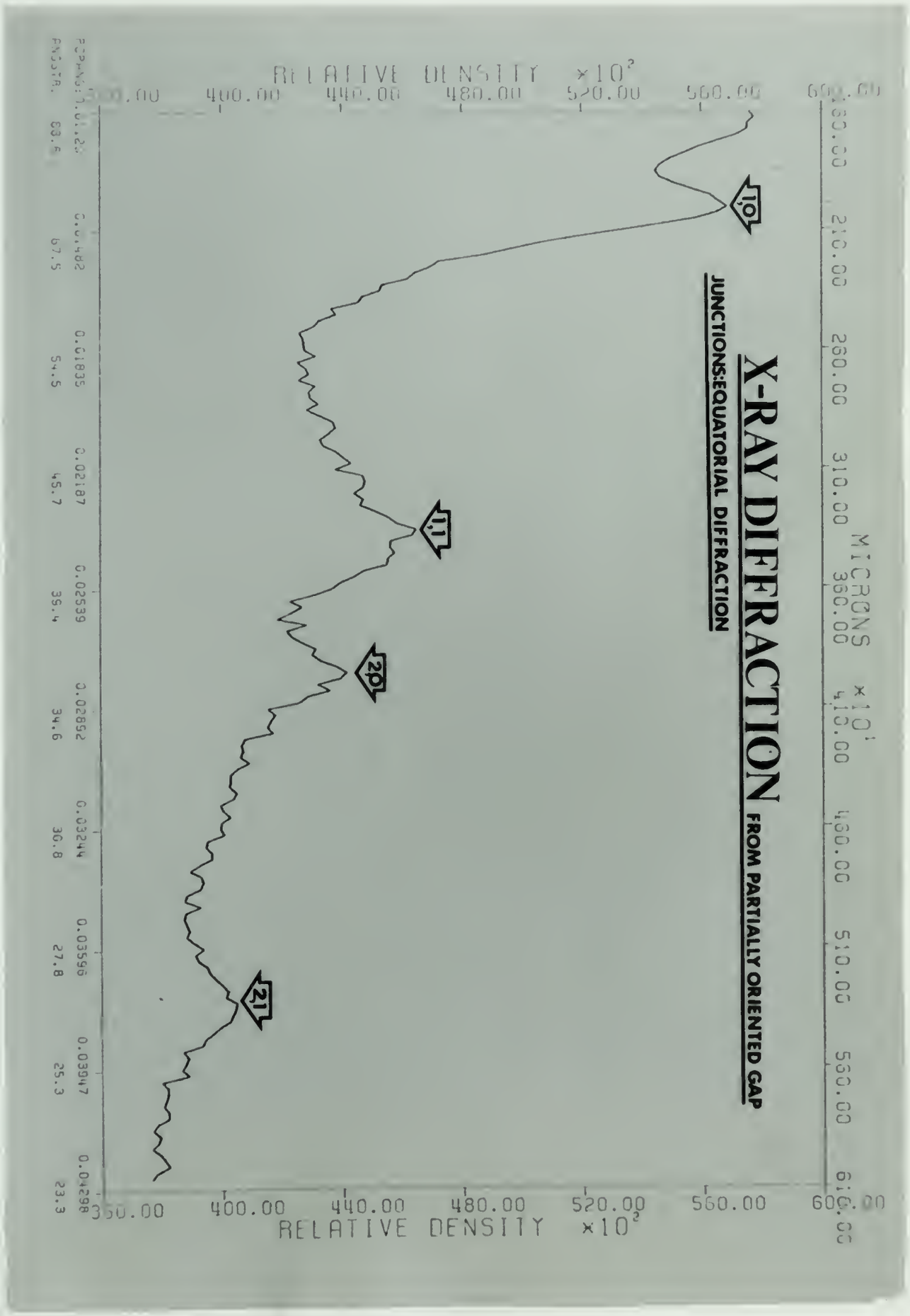
X-RAY DIFFRACTION FROM PARTIALLY ORIENTED GAP
JUNCTIONS:EQUATORIAL DIFFRACTION
RELATIVE DENSITY ×10²
MICRONS ×10¹
RELATIVE DENSITY ×10²
360.00
400.00
440.00
480.00
520.00
560.00
600.00
210.00
260.00
310.00
410.00
460.00
510.00
560.00
610.00
10
11
20
21

Plate 5

Figure 7

Shows a negatively stained gap junction displaying a pronounced tendency for curling-up on the edges. The arrow points at the edge-on view of the gap junction structure. Every connexon has an electron dense spot in the center that corresponds to the putative hydrophilic channel.


0.1µm

lattice. In the pellets of partially oriented gap junctions, all the rotational orientations of scatterers about the z axis are equi-probable. Hence, the observed equatorial intensity would be a circularly symmetric (averaged) function. The innermost equatorial arc was 1,0 reflection (Figs. 5 and 6) which corresponded to the six innermost hexagonal reflections in the optical diffraction pattern displayed in Fig. 4. The next arc corresponding to the 1,1 reflection was due to the next set of hexagonal reflections in the optical diffraction pattern.

The remaining two equatorial arcs corresponding to 2,0 and 2,1 reflections were related to the next two sets of hexagonal reflections, respectively, in the optical diffraction pattern. That the gap junctional lattice is hexagonal became evident upon the measurement of the spacings of these reflections. The diffraction pattern displayed in Fig. 6 could be indexed on a hexagonal lattice with lattice constant of 8.178 nm. The position of the reflection 2,1 departed slightly from that calculated, and was shifted to a higher radius.

3.3.2.3 Molecular Weight Determination by SDS-PAGE

The anionic detergent sodium dodecyl sulphate (SDS) is capable of dissociating complex enzymes, viruses and membranes into their constuent polypeptide chains (Weber and Osborn, 1975). Polyacrylamide gel electrophoresis in the presence of SDS yields the molecular weight dependent separation of polypeptide chains. Therefore SDS-PAGE has proven to be a very powerful analytic tool for investigating complex

Plate 6

Figure 8

A typical SDS-polyacrylamide gel electrophoretogram of gap junctions obtained form mouse liver. Gel was stained with silver stain; track A, standard proteins, the number shows mol. wt. = X 1000 daltons; B, gap junctional proteins displaying a prominent component of approximately 26,000 daltons (balck circle), and a diffuse component in approximately 43,000 dalton region (marked by a white arrow diffuse component could not be reproduced photographically); C, displays a band of α-chymotrypsinogen A of 26,000 mol. wt., that comigrates with the gap junctional polypeptide.

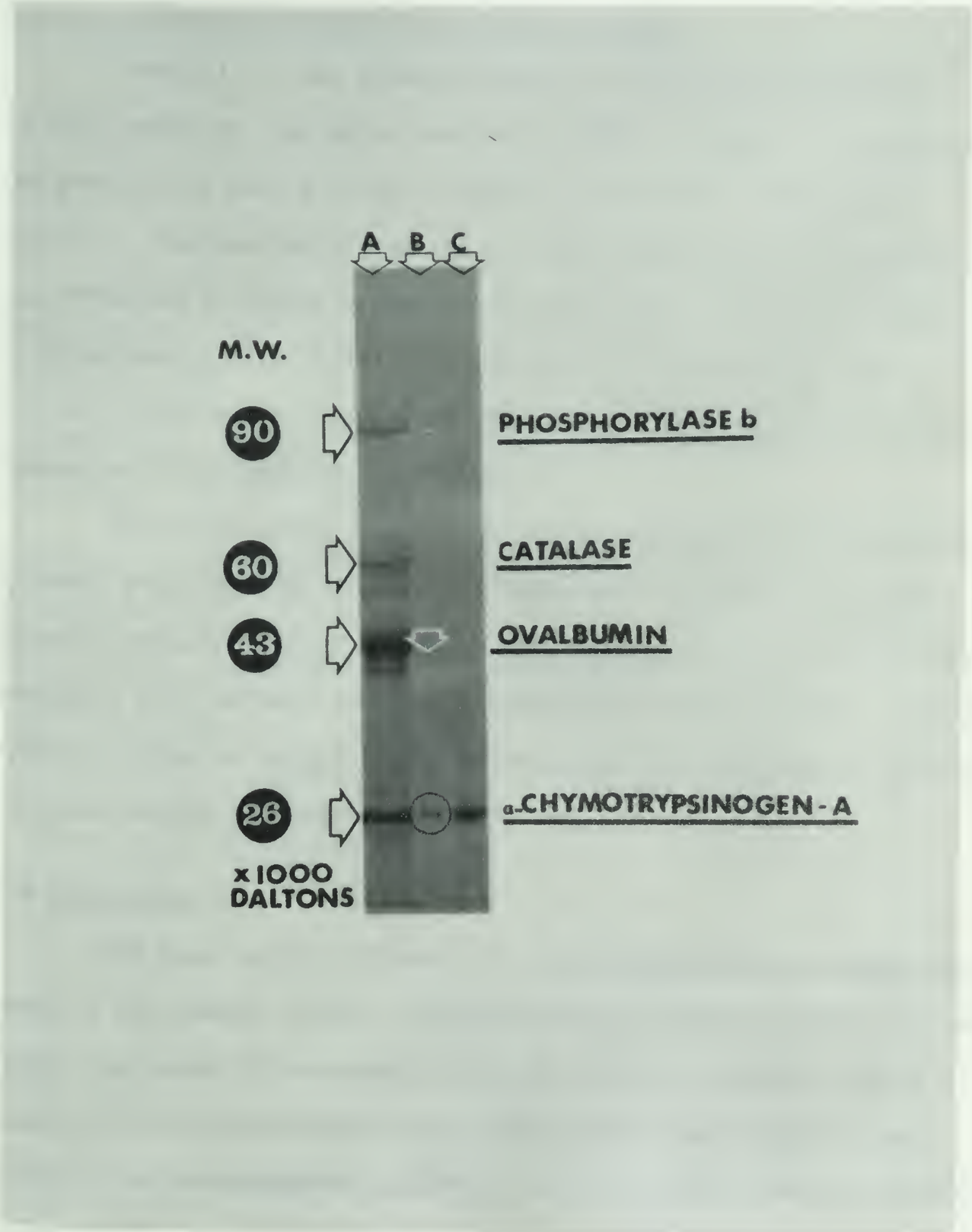
A
B
C
M.W.
90
PHOSPHORYLASE b
60
CATALASE
43
OVALBUMIN
26
α-CHYMOTRYPSINOGEN - A
x 1000
DALTONS

mixtures of membrane proteins. A detailed account of the theoretical considerations underlying the determination of molecular weights by SDS-PAGE is given in appendix "B".

3.3.2.3 Polypeptide composition of gap junctions

Initially it was observed that the conventional method of solubilization of samples by heating at 100°C for about 2-3 minutes in the presence of sample buffer failed to solubilize a substantial fraction. Whereas solubilization at room temperature for 30 minutes was effective in solubilizing most of the sample, as first pointed out by Henderson et al., (1979). In addition, the aggregation could further be reduced by running the SDS-PAGE immediately following the isolation of gap junction fractions.

The polypeptides comprising gap junctions as characterized by SDS-PAGE are displayed in Fig. 8. There was a predominant component of apparent molecular weight of 26000 which comigrated with α-chymotrypsinogen A with variable amounts of additional material in the 43000 apparent molecular weight region co-migrating with ovalbumin. No low molecular weight components were observed.

3.4 Discussion

The major problem inherent in the in vitro studies on gap junctions is the absence of any biological assay to evaluate the purity and assess the degree of preservation of the isolated fractions. This results from the insufficient information about their physiological role. As yet no endogenous activity, that could have been exploited in

developing some type of bio-assay, has been detected in the gap junctions. Therefore morphological criterion is the only assay for evaluating the purity and preservation of the isolated gap junctions. However, the morphological examination can only reveal gross-contamination by material of non-junctional origin and it does not serve as a sufficiently sensitive monitor of structural preservation.

The isolation protocol developed and described in detail in Section 3.2.2 produces exceptionally high yields of gap junctions (200-400 µg protein/40 animals) that compare well with a procedure due to Fallon and Goodenough (1981). The isolated fractions are morphologically highly enriched with gap junctions with very little amorphous contaminants. The gap junctions are relatively abundant in liver and occupy about 1.5% of the surface area of the rat liver hepatocyte membranes (Yee and Revel, 1978). About 200-400 µg of gap junctions can be obtained starting with 100-200 mg of plasma membranes/40 mice. Based on the approximation that the protein is uniformly distributed within the membrane, the recovery of gap junctions turns out to be of the order of 13% to 26%. The presence of 1 mM EGTA throughout the isolation protocol results in such high yields of gap junctions as first documented by Fallon and Goodenough (1981). The solubilization of non-junctional membrane is optimal at low ionic strength and slightly alkaline pH, which also eliminates potential contamination by otherwise detergent resistant uricase cores. The presence of EGTA at this stage avoids the aggregation of non-solubilized debris. The collagen fibres appear to undergo strong association with n-dodecanoyl sarcosine, an anoinic detergent employed for solubilizing the

the non-junctional plasma membranes. This binding presumably "swamps out" the intrinsic charge of collagen fibres and imparts an approximately constant negative charge per unit mass. These negatively charged collagen fibres serve almost like a "charged sieve" and trap most of the gap junctions, unless somehow removed. A low speed centrifugation (SS-34 rotor, 3100 rpm, 10 min.) is used to pellet down the collagen fibres, while the gap junctions still remain in the suspension.

The use of detergents to solubilize non-junctional membrane has been employed to advantage by others. The detergents employed for this purpose have included deoxycholate, Sarkosyl (NL-97), Triton X 100, Brij 58 and Lubrol WX (Benedetti and Emmelot, 1968; Zampighi and Unwin, 1979; Goodenough and Stoeckenius, 1972; Hertzberg and Gilula, 1979; Henderson et al., 1979; Fallon and Goodenough, 1981). In the present procedure, an anionic detergent n-dodecanoyl sarcosine is initially employed to solubilize most of the non-junctional plasma membrane (about 90-95% of the total protein). Subsequently treatments with non-ionic detergents Brij 35, Brij 58 and W-1 cause an increased solubilization of some of the gap junctional lipid and thereby induce closer packing of connexons as evidenced by a lattice constant that varies over 7.6-8.4 nm as compared to 8.0-8.8 nm observed in gap junctions isolated by using only sarkosyl (Caspar et al., 1977). Centrifugation in a sucrose step gradient finally yields the purified gap junctions. The presence of 1 mM EGTA and 0.1 mM 1-O-n-octyl- β-D-glucopyranoside (an non-ionic detergent) in the step gradient enhances the recovery and purity. The final preparation suffers from very little contamination by amorphous material.

Electron microscope images of negatively stained gap junctions display the characteristic hexagonal arrays of connexons. Each connexon is well-demarcated by the negative stain (uranyl acetate) located both at the center and at the perimeter. However, the stain is more accumulated at the center (six-fold axis of symmetry) than at the periphery thereby giving it an annular shape. The accumulation of stain at the six-fold axis is about 1.5 to 2.0 nm in diameter and corresponds to the putative hydrophilic channel. Lattice constant of the hexagonal arrays of connexons varies from approximately 7.6-8.4 nm as measured by optical diffraction analysis. In the high-dose electron micrographs of negatively stained gap junctions, the diffraction patterns extend to 2,0 reflection (except in a few cases where the diffraction patterns extends out to the 3,0 reflection). It appears as if the increased solubilization of some gap junctional lipid upon prolonged treatments with detergents results in greater close-packing of connexons. The potential of these gap junctions of providing high-resolution structural information by low-dose electron imaging techniques is yet to be explored.

A more objective estimate of the lattice constant of these gap junctions has been obtained by X-ray diffraction, which revealed a lattice constant of 8.2 nm. All the equatorial reflections could be indexed on a hexagonal lattice extending out to 2,1 reflection which appears to be slightly shifted to a higher radius from its calculated position. A similar observation has also been made by Makowski et al., (1977) in their original analysis of X-ray diffraction from partially oriented gap junctions. They attributed to it "strong diffraction

falling slightly off the equator on the lattice line corresponding to the 2,1 reflection". However, a detailed explanation emerged only after a three-dimensional map of gap junction at 1.8 nm was calculated by Unwin and Zampighi (1980) who analysed the low-dose electron micrographs of negatively stained gap junctions by Fourier methods. The continuous variation of amplitude and phase determined along 1,2 reciprocal lattice line calculated after collecting the three-dimensional data, revealed that this line was peaked away from equator. And the transition onto the second "B" form of gap junctions (presumably in an uncoupled state) rendered the off-axial peaks on 1,2 and 2,1 lattice lines into a single peak on the equator. Whereas the equatorial peak on 1,1 lattice line changed into two slightly off-axial ones, upon transition (Unwin and Zampighi, 1980). Electron images of gap junctions displayed that the connexons are linked in pairs. Since the two units of a pair were generally considered to be equivalent, they must be related by a two-fold axis parallel to the plane of gap junction at the middle of the gap. Since each connexon had six-fold rotational symmetry and the pair were spatially disposed with their six-fold axes coincident, the assembly had a point group symmetry 622 (having six two-fold axes perpendicular to the six-fold axis). Upon arraying these units in a hexagonal lattice with the effect that all two-fold axes lined up, a two-dimensional plane group P622 was generated (Caspar et al., 1977; Unwin and Zampighi, 1980). However, the amplitude and phase curves displayed minor deviations from the symmetry expected of the space group P622. Consequently the two halves of gap junctions disposed oppositely were considered to be only nearly equivalent (Unwin

and Zampighi, 1980). This conclusion was supported by quite symmetrical optical diffraction patterns obtained from the electron micrographs of negatively stained gap junctions, which displayed equally strong 2,1 and 1,2 reflections, having nearly the same phases.

Some gap junctions displayed a marked propensity for curving up and even to vesiculate. These gap junctions fortuitously provided the edge on views in a direction nearly parallel to the plane of gap junctions. These views also provided the variations along 1,1 and 0,0 lattice lines (Unwin and Zampighi, 1980). The connexons appeared to bridge the two apposed plasma membrane separated by a 2 nm gap. The transjunctional densities visualized in the edge-on views of gap junctions initially stimulated a number of attempts to interpret them. Goodenough (1976) and Hertzberg and Gilula (1979) have attempted to correlate these densities with the aqueous channels running across. Recently, Zampighi et al., (1980) have studied the distribution of stain within rat liver gap junctions visualized by thin sectioning and negative staining. The stain appeared to accumulate around the connexons in the extracellular space between the apposed plasma membranes. The other location permeated by the stain existed along the axis of each connexon, measures 1-2 nm in diameter and 4-5 nm in length, and it was restricted to the gap region. Only very rarely, thin linear electron densities hardly distinguishable seemed to traverse the entire width of gap junctions. It seemed evident that a hydrophilic cavity existed along the six-fold axis of connexon limited to the gap region in most of the cases. To what linear extent did this cavity extend further along the axis of connexon, remained uncertain.

What causes the curvature in the gap junctions? It is evident that in case of the curved gap junctions, the paired connexons can only be related by local two-fold axis (Caspar et al., 1977). Treatment with trypsin has been reported to induce the formation of vesicles or curved sheets (Goodenough, 1976). In general, the proteolysis of the gap junction fractions has been claimed to be an important factor in generating vesiculated forms. The gap junctions isolated by Zampighi and Unwin's (1979) method display no detectable sign of proteolysis as evidenced by SDS-polyacrylamide gel electrophoretic analysis of the isolated fractions and they also appear to lie as flat sheets on the grids. Recently, Baker et al. (1983) have claimed that the gap junction's two halves are non-equivalent. They have studied gap junctions isolated from mouse liver following the procedure due to Fallon and Goodenough (1981) by low-dose electron microscopy of negatively stained preparations. The projected images of hexagonal gap junctional lattice display skewed hexameric connexons. This skewing of the hexameric connexons has been taken to suggest that the pair of hexagonal arrays of connexons that form the gap junction may be structurally non-equivalent. These preparations have suffered endogenous proteolysis as documented by SDS-polyacrylamide gel data. Clearly, proteolysis may play a role in inducing the formation of curved sheets of gap junctions. But the role played by the detergent used for isolation and lipids intrinsic to the gap junctional bilayer has not as yet been studied. It has been reported that lyotropic detergents may exert a pressure for increasing curvature in the bilayer on account of their "wedge" shaped structure (Haydon and Taylor, 1963) and may thus result

in the generation of smaller mixed micelles. Whereas bile salts may "chop up the bilayers" into disc-like fragments with bile salt molecules lining up on the hydrophobic edges (Helenius and Simons, 1975) (see appendix "A"). The gap junctions isolated by employing the present isolation procedure do not detectably suffer from endogenous proteolysis, and yet some of them display marked curvature. Perhaps it is a consequence of using lyotropic detergents as discussed above. Yet another factor which may be potentially responsible for inducing the curvature is the degree of selective removal of lipids by various detergents.

These possibilities demand further experimental verification to elaborate their respective role(s).

The characterization of the number and the molecular weight(s) of the constituent polypeptides of gap junctions has been a subject of much debate. The present isolation protocol eliminates the use of exogenous proteases and treatment with urea. Furthermore, protease inhibitors such as phenylmethyl sulphonyl fluoride and p-chloromercuribenzoate were always employed. In SDS-polyacrylamide gel electrophoresis these gap junctions display a predominant component of apparent molecular weight (Mr) 26,000 and a slower running component of 43,000 Mr represented by a broad diffuse band. Henderson et al., (1979) have analysed the polypeptide composition of mouse liver gap junctions isolated by a nonenzymatic protocol involving the solubilization of non-junctional plasma membrane by Triton X 100. They described two components; a major component of Mr 26,000 and a minor component with an 21,000 Mr. They also resolved components of Mr 45,000 and 50,000 respectively.

Some broad diffuse bands in the region of Mr 70,000-80,000 and 90,000-110,000 Mr were also discernible. An important characteristic of these two Mr 26,000 and 21,000 components has been described by Henderson et al. (1979). These two components displayed a strong propensity to form multimers in SDS; initially they formed only homodimers but with time they formed multimers too. Heterodimer formation was never observed. The aggregation of these components in SDS is enhanced upon heating generally used for achieving solubilization. This observation has a profound implication in attempting to rationalize the often conflicting literature on the gap junctional polypeptides. Therefore it seems reasonable to assume that the 43,000 Mr is a dimer of two 21,000 Mr polypeptides. Hertzberg and Gilula (1979) have observed a Mr 27,000 component together with a broad diffuse band in the Mr 47,000 region. The diffuse Mr 47,000 band appeared to have several discrete protein bands in this molecular weight range. Attempts to demonstrate the glycosylation of these components have always yielded negative results. A number of workers have reported on the existence of a 27,000 Mr polypeptide as a major component of gap junctions (Duguid and Revel, 1975; Dunia et al., 1974). Based upon studies on mouse hepatocyte gap junctions, Culvenor and Evans (1977) have concluded that all the components with molecular weight less that 38,000 Mr are due to proteolysis. However, in view of the fact that these authors could not obtain highly enriched fractions of gap junctions in the absence of proteolysis, this claim appears to be unreliable and probably more so in the face of a large number of bands resolved on their gel that renders such an absolute assignment arbitrary. Similarly it is difficult to explain

the results of Ehrhart and Chauveau (1977) who have reported that a 34,000 Mr component was the only component present in morphologically enriched gap junction fractions obtained using collagenase. Perhaps this has been caused by both the proteolysis and the aggregation of the resulting polypeptide(s) in SDS. Zampighi and Unwin (1979) have reported a 30,000 Mr component as the constituent polypeptide of gap junctions isolated from rat liver using deoxycholate and Lubrox WX. The higher molecular weight components, probably representing aggregates, were also observed. Finbow et al., (1980) have provided further support for the notion that the major gap junctional polypeptide has a molecular weight of 26,000 Mr (from rat liver).

Recently Nicholson et al. (1981) have carried out peptide mapping and partial sequencing of the NH_2-terminal 52 amino acids of a gap junctional polypeptide of molecular 28,000 Mr. Two-dimensional peptide mapping has indicated that all of the polypeptides present in the purified gap junction fractions are derived from 28,000 Mr polypeptide except for the contaminants which can be recognized. Upon treatment with trypsin this is reduced to two 10,000 Mr peptides which are highly hydrophobic as judged by peptide-mapping and amino acid analysis. Since the COOH terminal is susceptible to proteolysis by trypsin, it must be localized at the cytoplasmic face. On the other hand the NH_2 terminal remains unaffected and therefore it must be inaccessible to trypsin. The NH_2-terminus sequence of 52 residues displays a highly hydrophobic stretch of 18 residues after initial uncharged 14 residues, interrupted by a single charged Arg-32 and

flanked at the NH_2 terminus by three basic residues and at the COOH terminus by three acidic residues.

The gap junctional polypeptide(s) has a rather short half-life in comparison to other plasma membrane proteins from liver which turnover slowly. The half-life of a 21,000 Mr polypeptide from mouse liver gap junctions has been reported to be 5 hours (Fallon and Goodenough, 1981). Such a rapid turnover has been implicated in the regulation of intercellular communication at the level of protein synthesis and breakdown rather than a reversible physical opening and closing of channels at the level of individual connexons.

3.5 Epilogue

3.5.1 A Speculative Discourse on the Secondary Structure of Connexin

In the absence of any detailed three-dimensional structure of the low resistance channels at molecular level, the nature of the secondary structure(s) sustaining the channel architecture can only be speculated. In case of the integral membrane proteins, the requirement for maximizing hydrogen bonding can be satisfied only when the regions of polypeptide chain which interact with the lipid hydrocarbon domain adopt regular secondary structures. Three types of regular secondary structure are accessible to the membrane intercalated portion of integral membrane proteins: the α-helix, the β-pleated sheet and the β-helices (Kennedy, 1978). The presence of α-helices in the gap junction has been reported by Makowski et al. (1977) based upon the results

of X-ray diffraction studies on partially oriented preparations. A broad band of continuous intensity at about 1 nm spacing on the equator was considered as a diagnostic feature for the presence of α-helices oriented within 20° of the perpendicular to the plane of the gap junction. Later on Makowski et al. (1982) have claimed the presence of cross- β conformation in the gap junction protein. This assignment was based upon the presence of strong diffraction centered at 0.47 nm spacing on the meridian, and at approximately 1 nm spacing on the equator. In the cross- β conformation, the polypeptide chain direction is transverse to the fibre-axis (Fraser and MaRae, 1973) and in case of the gap junction it implies that the chain direction is parallel to the plane of the junction. Cross- β conformation has also been reported in the phage T4 tail fibres (Earnshaw et al., 1979) where it facilitates the formation of structurally rigid dimers. That the regions of β-sheet possess a strong propensity for pairing is demonstrated by the structures of concavalin A (see the concavalin A dimer structure, Reeke et al., 1975), tomato bushy stunt virus (which displays the dimer contacts between the tomato bushy stunt virus coat protein subunits, Harrison et al., 1978) and the phage T4 fibre (Earnshaw et al., 1979). It has been argued (Earnshaw et al., 1979) that this potential for pairing is inherent in β-pleated sheets due to two structural peculiarities. First, the extended flat structure of the sheets offers only small steric hindrances and facilitates packing by affording to make many more contacts in the packed sheets. Second, the β-pleated sheets are sided in that they have a front and a back and tend to have a hydrophobic side and a hydrophilic side, a configuration that would

facilitate pairing (Earnshaw et al., 1979). The implication for the structure of the gap junction is evident as the channel is formed by the connexon pair disposed with their six-fold axes coincident and related by a two-fold axis parallel to the plane of the gap junction. The application of Chou and Fasman's (1974) algorithm permits the prediction of the secondary structure from primary sequences. Such an application to the known sequence of 50 NH_2 terminal amino acids in connexin, reveals the possibility of a β-pleated sheet conformation in the hydrophobic region of the protein (Nicholson et al., 1981). If the secondary structure of the connexin is of β-pleated sheet type, only 15 residues would be required for spanning the lipid bilayer and only one charged Arg-32 would have to be buried in the hydrophobic region (Nicholson et al., 1981). However, the charged residues can participate in the transmembrane ion-pair formation with the residues of other strands (Englemann et al., 1980). At present these models are speculative. Besides, Chou and Fasman algorithm for predicting the secondary structure is based upon the data derived from soluble proteins and hence is liable to make spurious predictions in case of the integral membrane proteins as evidenced by its application to *E. coli* protein I (Chen et al., 1979).

β-barrels can accommodate as few as 5 and as many as 13 strands; and their cross-section remains more or less invariant regardless of the strand number due varying of strand twist around the barrel (Richardson, 1981). An interesting 8-stranded parallel β-barrel composed of straight helical chain has been documented by Salemme and Weatherford (1981a): the crossing polypeptide chain conformations have

been adjusted to generate a structure whose inherent twist produces the required cylindrical pitch and curvature. There is no appreciable effect on the quality of interchain hydrogen bonds. The diameter of this cylinder is approximately 1.6 nm, a figure close to the size of gap junctional aqueous channel as determined by flourescent tracer methods (Loewenstein, 1981). However, the interiors of β-barrels of water soluble proteins have been found to be packed with hydrophobic side chains, a feature that would be difficult to reconcile with their presumed role of functioning as aqueous channels in the biomembranes.

4. IN SITU STRUCTURAL STUDIES

4.1 Introduction

The extent of intercellular coupling mediated by gap junctions is susceptible to a number of factors that perturb the intracellular milieu. For instance, coupling is extremely labile in the face of cell injury (Loewenstein, 1981); and procedures involving changes in cell metabolism are likely to abolish coupling rapidly. Since the isolation procedures involve homogenization of the tissue as the very first step (which breaks the tissues and ruptures the cell membranes) it is reasonable to ask if the isolated gap junctions differ in anyway from their *in situ* counterparts. A number of workers claim that the connexons in the isolated gap junctions are in their closed state (uncoupled; Peracchia, 1980; Makowski et al., 1982). For example, an analysis of gap junctions suspended in 50% sucrose by employing lowangle x-ray diffraction has shown that sucrose can easily enter into the extracellular gap but fails to enter into the channel. This evidence has been taken to suggest that the isolated gap junctions in this study are in an uncoupled state (Makowski et al., 1982). Obviously, a greater understanding of the structural dynamics of these communicating channels can be availed by a knowledge of their *in situ* structural configurations as a function of various physiological effectors. The freeze-fracturing technique is unique in providing the structural correlates of various functional state(s) of gap junctions (Peracchia, 1980). It has been demonstrated that the treatments that uncouple the gap junctions also induce the intramembranous particles (corresponding

to the connexons) to pack into tight and more crystalline arrays (Peracchia, 1980). However all these studies have employed the conventional chemical fixation (usually with glutaraldehyde) and cryoprotective treatment (with glycerol). Treatment with chemical fixatives may not preserve the in situ state of the molecules in biomembranes. Besides, glutaraldehyde fixation has also been shown to uncouple the cells, as monitored by electrophysiological methods (Bennett et al., 1972). Therefore, it remains to be determined if the glutaraldehyde fixation causes any structural changes in the gap junctions. Even the conventional methods of freezing at -150°C do not arrest the molecular motions during cooling and hence may allow molecular rearrangements (Costello et al., 1982).

In order to avoid the possibility of artifacts caused by both the conventional freezing and the chemical fixation (by glutaraldehyde), the technique of rapid freezing (Van Harreveld et al., 1965) has been employed in the present study to investigate the connexon substructure in situ. Rotary shadowing in combination with rapid-freezing and freeze-fracturing has proven valuable in resolving the subunit structure of connexons. This has also permitted an enquiry into the effect of glutaraldehyde fixation on the structure of the gap junctions.

4.2 Materials and Methods

4.2.1 Freeze-Fracturing and Etching:

Small pieces of liver from 2 month old albino mice were quickly frozen within approximately 30 seconds, without any chemical fixation

or cryoprotection, by dropping them onto a polished silver block cooled to about <-196°C by liquid N_2 (Van Harreveld et al., 1965). The rate of cooling in this technique is very fast compared to that when the material is frozen by immersion in liquid coolants. The reason for this difference lies in the fact that the metals have a higher thermal diffusivity than liquids and do not volatilize to form insulating gaseous jackets around the specimen (Heuser et al., 1979; Carlsaw and Jaeger, 1974). Frozen tissue pieces were transferred to a Balzers BA 360 M high vacuum freeze-etching apparatus (Balzers AG, Liechtenstein) equipped with an electron-beam evaporation unit and a quartz-crystal for monitoring the film thickness. Samples were freeze-fractured and etched at -100°C for 2 min. at a vacuum of 2×10^{-6} torr or better. Rotary shadowed replicas were prepared according to the standard methods (Margaritis et al., 1977; Tewari and Malhotra, 1978). Platinum-carbon was evaporated (at 30° angle) so as to cause a frequency shift of 400 Hz in a quartz-crystal monitor. This corresponds to a film thickness of about 4.5 nm (electron beam evaporation equipment EVM 052 with electron beam gun EK552, operating instructions BB 200048 BE, Balzers, Liechtenstein, p.1-18).

To study the effect of fixation, pieces of mouse liver were fixed with 2.5% glutaraldehyde in 0.1 M cacodylate buffer (pH 7.4) at room temperature for various time intervals and thereafter rapid frozen and freeze-fractured as described above. For conventional freeze-fracturing, the pieces of liver were infiltrated with glycerol (25%) in 0.1 M, cacodylate buffer (pH 7.4) after fixation in glutaraldehyde. Samples were frozen in liquid Freom 22, transferred to liquid N_2 and

then freeze-fractured as described above. For comparative purposes, fixation with 2.5% glutaraldehyde in phosphate buffer (pH 7.4) was also investigated.

4.2.2 Electron Microscopy:

The replicas were examined in a Philips EM 300 or a EM 400 T electron microscope equipped with a goniometer stage and operated with a liquid N_2 cooled anticontamination device.

All the electron micrographs were enlarged to the same final magnification before any measurements were made. A Carl Zeiss digital image analyzer (MOP-3) was employed for the measurement of centre-to-centre spacings between the connexons (at a final magnification of 332,000X). Centre-to-centre distances between the adjacent connexons (generally nearest neighbours along the three directions at approximately 120° to each other) were measured. A distribution analysis program of MOP-3 was used to calculate the arithmetic mean and standard deviation and the frequency distribution of the interconnexon spacings.

4.2.3 Rotational Filtering:

For the analysis of the rotational symmetry of connexons, the electron micrographs of connexons (original magnification 63,000 to 80,000X) were photographically enlarged and printed on film in reverse contrast. These negatives were then used to evaluate the rotational symmetry of connexons by Markham's rotational filtering technique (Markham et al., 1963).

4.3 Results and Interpretation

4.3.1 Background to the Interpretation of Results

4.3.1.1 The Case for Physical Fixation by Freezing

During the process of freeze-fracturing, a frozen sample is fractured and a Pt-C replica of the fracture face is prepared while the sample is still in the frozen state. In freeze-etching, the fracturing is followed by etching in which some of the ice is sublimed away. In the conventional freeze-etching, chemical fixatives (multifunctional cross-liking agents such as glutaraldehyde) are employed to arrest the detailed molecular organization of the native specimen. However this treatment may not altogether eliminate the possibility of molecular rearrangements and conformational changes. It is simply due to the fact that all the molecular species would not be simultaneously equally reactive towards the cross-linking agent. Also the conformational changes would occur inevitably in some molecules upon cross-linking. In freeze-etching, the chemical fixation is substituted by freezing. However, during freezing, structural changes could be produced as a result of growing ice-crystals. By employing cryoprotectants (such as glycerol) ice crystal growth is significantly reduced, but the cryoprotectants themselves may induce structural and physiological changes. In aqueous or hydrated specimens during freezing a random dispersion of ice crystals is formed. Ice crystal growth progresses at the nucleation points at the expense of water drawn from the surrounding medium. This causes an increase in solute concentration in the regions between growing ice crystals. Finally, when the solute concentration in these regions has increased up to a certain level, an amorphous solid eutectic is given rise to (and the ice crystal growth comes to a halt

altogether), made up of water and solute in a glassy (vitrified) state (Wilison and Rowe, 1980). Ice crystal growth has been demonstrated to continue to occur in the pure water at tempertures down to approximately -130°C, but ceases at temperatures lower than this. In solutions having the same solute content as is usually encountered in the living organism, the temperature range over which ice crystallization takes place is from about -20°C to -80°C (recrystallization point). The growth of ice crystals is a function of a variety of factors including the solute concentration and the cooling rate to the recrystallization point. When the cooling rate and/or the solute concentration increase, the resulting ice crystals produced are smaller in size. As mentioned before, as the solute concentration increases beyond a certain critical value the whole system solidifies as an amorphous eutectic. The ice crystal nucleation is governed by the rate of cooling. Heterogeneous ice crystallization which involves solute molecules as the likely nucleation sites, has been shown to occur at slow cooling rates. Whereas homogenous ice crystallization in which water molecules are represented as the potential nucleation sites occurs upon faster cooling. The uniformly sized ice crystals formed at sufficiently high cooling rates reach a minimum value of dimensions of about 20 nm^3 (Willison and Rowe, 1980). Moore (1973) has identified this process as 'vitrification'. However, vitrification is very difficult to achieve in practice because regardless of how effective a freezing method is employed, the rate at which the heat can be conducted out of the specimen is still the most important limiting factor (Sleytr and Robards, 1982). Although a high heat transfer coefficient

at specimen/coolant interface is a necessary prerequisite for the high rate of cooling, still the main restrictive factor to rapid cryofixation is the inherent low thermal conductivity of water. Complete vitrification has only recently been attained within a bulk liquid water specimen (Bruggeller and Mayer, 1980; Bruggeller and Meyer, 1982). The aim of cryofixation in the ultrastructural studies is to minimize the size of ice crystals formed. The maximum size of ice crystals that can be tolerated would depend upon the resolution sought and since Pt-C replicas are inherently limited in resolution to about 2 nm (due to the grain size), ice crystal growth should be limited in dimensions less than this (Sleytr and Robards, 1982).

4.3.1.2 Conventional Freezing

In the conventional method of freezing, first introduced by Moor and Muhlethaler (1963), the specimen is first frozen by rapid immersion in Freon 12 (dichlorodifluoromethane) at its melting point (-158°C). Freon 13 and Freon 22 (monochlorodiffluromethane) were introduced later, and are equally effective.

After freezing in liquid Freon, the specimen is quickly transferred into a container filled with liquid N_2. The cooling rates are different in different regions of the sample (peripheral regions are usually best preserved) and do not vary linearly with the time (Bald and Robards, 1978; Van Venrooij et al., 1975). Cooling rates appear to vary with the employed techniques from 100-1000°C per second (Costello and Corless, 1978; Van Venrooij et al., 1975).

4.3.1.3 Rapid Freezing

In a method originally due to Van Harreveld and Crowell (1964) freezing in liquid coolants is dispensed with and instead use is made of the higher thermal diffusivities of metals as compared to fluids (Carlsaw and Jaeger, 1974). Freezing is achieved by directly placing the specimen against a silver block (with polished surface), cooled with liquid N_2 to -196°C. Freezing is usually accomplished in a few milliseconds. This method was further developed by Heuser and co-workers (reviewed in Heuser, 1981) who substituted liquid N_2 with liquid helium (He) and thus were able to cool the block of metal (copper) down to -269°C. This produces an ultra-rapidly frozen layer of approximately 5 - 15 m thickness at the specimen surface in contact with the cold metal.

There are two other methods in existence, which have also been claimed to produce equally better preservation by ultra-rapid freezing of the thin specimen clamped between conducting metals. The "jet freezing" method involves spraying of propane on the opposite sides of compressed specimen (Mueller et al., 1980), whereas the "sandwich" method (Costello, 1980; Costello et al., 1982) employs freezing of the specimen clamped between two thin strips of copper foil by dropping it into liquid coolant. Recently Costello et al., (1982) have measured the cooling rates for all these three methods by using minute thermo-couples housed in the samples. The cooling rates appear to be greater than 10^4 K/s. In this context it is instructive to note that the theoretical cooling rate required to vitrify the water is in the excess of 10^4 K/s (Franks, 1980). It appears that all these three methods

are capable of providing well-preserved cryofixed biological samples with no signs of ice-crystal damage in the peripheral few micron thick region.

4.3.1.4 Interpretation of Freeze-Fracture Replicas

Branton (1966) was the first to recognize that during the process of freeze-fracturing, the fracture plane passes through the hydrophobic interior of the biological membranes, so that the inner faces are exposed. Fracture faces usually reveal particles of approximately 10 nm diameter, their number being subject to variation from one membrane type to the other. It was proposed that the particles are true features of the membrane interior (Branton, 1971). It was noticed that upon etching, fractured membranes usually displayed a narrow ridge approximately 3 nm thick. This ridge was observed to be continuous with one of two parallel ridges, at the transition of face view into a cross-fracture, that are responsible for the usual appearance of cross-fractured membranes. These observations lent support to the notion that the membrane was split. The fracture faces of swollen nerve myelin, rod outer segment membranes and swollen lecithin lameller phases (Branton, 1967; Clark and Branton, 1968; Staehlin, 1968) were subsequently interpreted using similar reasoning. A consideration of the actual dimensions and spacings of the ridges soon led to the conclusion that there ought to be an 5.5 nm-wide gap between them. Radioactively labelled bilayers and multilayers were assembled by employing the classic Langmuir-Blodgett technique (Langmuir, 1917; Blodgett, 1935; Langmuir, 1939). After freezing, these were fractured and the split

layers were assessed for radioactivity content. The results obtained after such an analysis can be reasonably explained only after assuming that the assemblies fracture along a plane defined by the terminal methyl groups of the individual monolayers (Deamer and Branton, 1967). Upon shadowing, fracture faces displayed very smooth surfaces devoid of any particulate projections. Similar observations have also been reported in the cases of membranes which have no or little protein. For instance, relatively smooth fracture faces have been noted in the lameller lipid phases (Deamer et al., 1970), liposomes (James and Branton, 1971) and nerve myelin (Branton, 1967; Malhotra et al., 1975). This hypothesis was further strengthened by the observation that aldehyde fixation, which cross-links proteins, rendered the appearance of the membranes unaffected after freeze-fracturing. There was only an enhancement in the overall mechanical stability (Jost, 1965; Branton and Park, 1967; Tillack and Marchesi, 1970). However, subjecting these membranes to lipid extraction, prior to aldehyde fixation, abolished the splitting of membranes upon freeze-fracturing (Park and Branton, 1966; Fleisher et al., 1967; Branton and Park, 1967). These experiments emphasized the crucial requirement of lipidic regions to accomplish freeze-fracturing of biomembranes. Deamer and Branton (1967) have propounded an hypothesis to explain the splitting behaviour of biomembranes in freeze-fracturing. Their proposal rests on Kauzmann's (1959) thermodynamic considerations of the temperature dependence of hydrophobic bonding. Since the strength of hydrophobic 'bonding' decreases with the decreasing temperature the hydrophobic interior of

of the biological membranes would be most susceptible to splitting upon freeze-fracturing at the center of the lipid-bilayer.

Another line of evidence in support of the membrane splitting hypothesis has come from experiments involving membrane-surface markers (attached F-actin or covalently linked Ferritin) that have demonstrated that these markers can only be observed after etching. Fracture faces never displayed these markers (Pinto de Silva and Branton, 1970; Tillack and Marchesi, 1970). That both the fracture faces of a membrane can not be etched ('unetchable') was demonstrated by employing the complimentary replica techniques (Sleytr, 1970; Wehrli et al., 1970; Chalcroft and Bullivant, 1970). This observation too, can only be reconciled with the membrane splitting hypothesis.

Branton (1967; 1971) has suggested that the molecular correlates of membrane-intercalated (or intramembranous) particles, displayed on the freeze-fracture faces of biomembranes, are membrane proteins. They represent integral membrane proteins and their 'attendance' on the fracture faces is modulated by the metabolic activity of a cell or membrane type (Bretscher and Raff, 1975).

4.3.1.5 Nomenclature

In 1975, Branton et al. proposed a unifying system of nomenclature for labelling the freeze-fractured surfaces. When the plasma membrane is fractured, it splits into two halves. One physical half of this membrane retains contact with the underlying protoplasm and the other half is in contact with the extracellular matrix. That fracture face of the cleaved half of the membrane which still retains contact

with the protoplasm is labelled as protoplasmic face (P face), and the other fracture face which is associated with the extracellular matrix is correspondingly labelled as extracellular face (E face).

4.3.1.6 Artifacts Induced upon Fracturing - The Plastic Deformation

By using morphologically and chemically well-defined biological and non-biological polymers, frozen and embedded in an ice matrix, significant information has been gained concerning the mechanics of fracturing (Dunlop and Robards, 1972, 1973; Sleytr and Robards, 1977). Fracturing profiles have been reported to be temperature-dependent and, even at 4° K, plastic deformation has been observed in some polymers (Sleytr and Robards, 1977). In principle, when the fracturing is carried out at temperatures much lower than the bulk polymer glass transition temperature (Cowie, 1973), no plastic deformation should be observed. But, plastic deformation has been reported in the polymer spheres (fractured at temperatures far below their bulk polymer glass transition temperature), it is therefore only reasonable to assume that the temperature of the spheres must have risen above the glass transition point. Therefore, it is obvious that during the fracturing process considerable energy must have been dissipated as heat (Sleytr and Robards, 1982). Deformation profiles so far studied for most globular polymers seem to follow a general pattern. Upon the arrival of a propagating brittle fracture plane (Van Buern, 1960) at a potentially deformable globular polymer it may be deformed in such a fashion that one half may stay completely embedded in the surrounding ice matrix

whereas the other half may be pulled out to form an elongated cone-like protrusion (Sleytr and Robards, 1982).

A glimpse into the deformation process is afforded by comparison of the volumes of cone-like deformation and roughly spherical depression on the opposite complimentary face which suggests the adiabatic expansion of the globular polymer (Sleytr and Robards, 1982). Evidently, the heat transfer within the polymer, the surrounding ice matrix and through the polymer/matrix interface would govern the extent of plastic deformation of a globular polymer (whether it would be only partially or completely deformed). Following deformation, other secondary structural changes involving elastic recontraction or collapse or total degradation may occur. Plastic deformation caused by freeze-fracturing in ordered protein structures such as catalase crystals or cylinders of nucleosome-core particles has been well documented (Lepault and Dubochet, 1980). In case of the transmembrane protein (such as connexin) which are almost equally bonded to both sides of the lipid bilayer, there would be a disruption of covalent bonds and hence a lot of energy can be expected to be dissipated, upon fracturing. This would result in maximum deformation (Edwards et al., 1979).

Another source of deformation is the energy deposited in the specimen (thermal load) during replica deposition. Alterations in the three dimensional structure are feasible on account of the partial transfer of heat load into the entropy driven conformational changes. This heat dissipation may cause a variety of secondary changes ranging from a mild elastic recontraction to total degradation of the deformed material, being somewhat dependent upon the thermal conductance within the polymer.

Plate 7

Figure 9

Electron micrographs of freeze-fracture replicas of hepatocytes showing gap junctions printed in positive contrast.

a. Fracture with arrays of connexons (intramembranous particles) on the P-face (P) and complementary pits on the E-face (E).

b. Fracture with arrays of connexons on the P-face. Many of the connexons reveal a subunit structure and a central depression (arrows).

c. A connexon printed in reverse contrast. Note the 6 subunits surrounding a depressed area.

d. Markham's rotation of the connexon shown in Figure 9**c**. The image was rotated 5 times. Note the six-fold symmetry of the connexon.

e. Electron micrograph of a connexon printed in reverse contrast. Note the four subunits surrounding a depressed area. The two blank spaces (arrows) indicate that two subunits have been broken off during freeze-fracturing. In this electron optical projection the connexon appears to be flattened along the vertical axis.

f. Markham's rotation of the connexon shown in Fig.9**e**. The image was rotated 3 times. Note the apparent four-fold symmetry of the connexon.

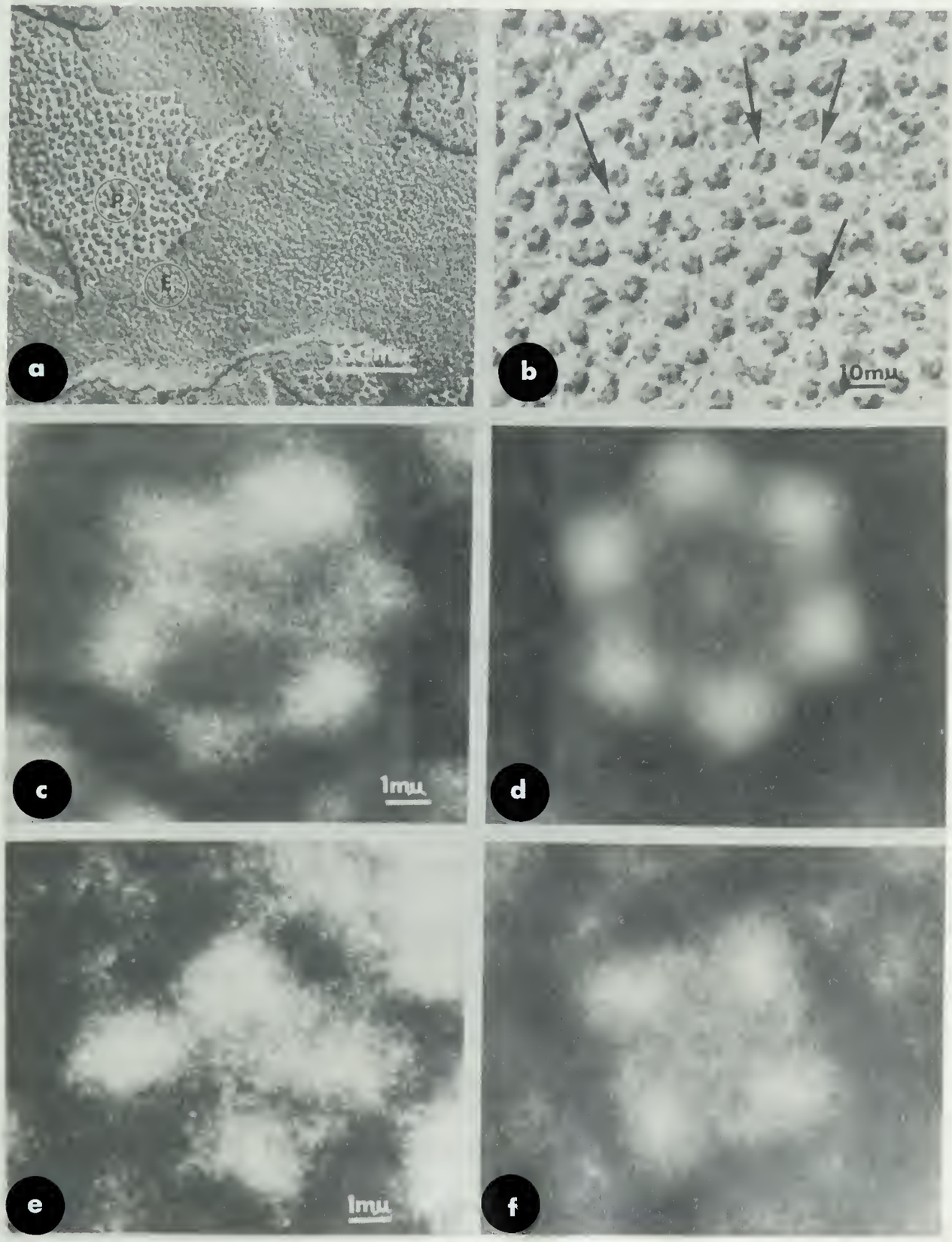
a
P
E
b
10mμ
c
1mμ
d
e
1mμ
f

4.3.2 Sub-unit Structure of the Connexons

The quasi-crystalline lattice of connexons in gap junctions is vividly displayed by the freeze-fracture technique. Rotary shadowed replicas of the unfixed, uncryoprotected and rapid frozen mouse liver gap junctions demonstrate a characteristic array of intramembranous particles corresponding to the connexons on the P face (Fig. 9 a) and the complimentary pits on the E face (Fig. 9 a). These connexons display no evidence of a lattice order, the hexagonal packing, which so typically characterizes the isolated gap junctions (Fig. 3). The average diameter of each connexon, after thickness correction (for Pt-C replica thickness), is approximately 6 nm which compares well with the diameter suggested by the correlated electron microscopic and x-ray diffraction studies (Makowski et al., 1977 and Caspar et al., 1977). Some connexons reveal six subunits (Figs. 9 b,c,e) while the rest display less than six subunits . Each connexon demonstrates a clear central depression (Figs. 9 b,c,e) which presumably corresponds to the "stain penetrable core", of the connexons observed by negative staining (Fig. 3) (Caspar et al., 1977; Unwin and Zampighi, 1980) and considered to be the opening of axial hydrophilic channel (Makowski et al., 1977; Unwin and Zampighi, 1980).

Markham's rotation (Markham et al., 1963) of the connexons indicates that some of them have a six-fold symmetry (Figs. 9 c,d). However, deviations from the six-fold symmetry are also frequently encountered. For example, some connexons display an apparent tetrameric symmetry (Figs. 9 e,f). A possible explanation of this tetrameric symmetry emerges when a model of the connexons (Fig. 10 a) is

Plate 8

Figure 10

a. A model of a connexon showing six subunits surrounding an axial depression.

b. The model shown in Fig. 10a photographed at an angle of about 30°. Note the superimposition of some of the subunits. The connexon appears to be flattened along the vertical axis. If the two subunits (arrows) were missing the projection would be very similar to that shown in Fig.9**e** .

c. Markham's rotation of the model shown in Fig. 10b. The image was rotated 3 times. Note the apparent four-fold symmetry of the model.

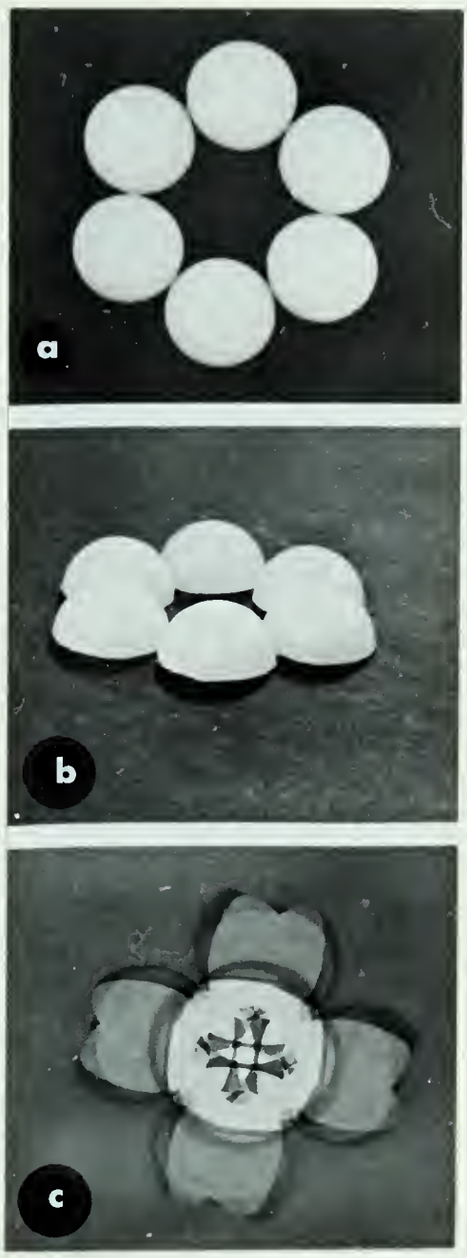
a
b
c

Plate 9

Figure 11

a. An array of connexons photographed at 0° (Fig. 11a) and after tilting for 30° (Fig. 11b). Note the change in electron optical projections of the connexons (corresponding large and small arrows and arrowhead). The connexons which appeared to be symmetrical and showed substructure (Fig. 11a) have become flattened and do not show a clear substructure after tilting (Fig. 11b).

c. An array of connexons photographed at 0° (Fig. 11c) and after tilting for 30° (Fig. 11d). Note the change in projections of the connexons (arrowhead).

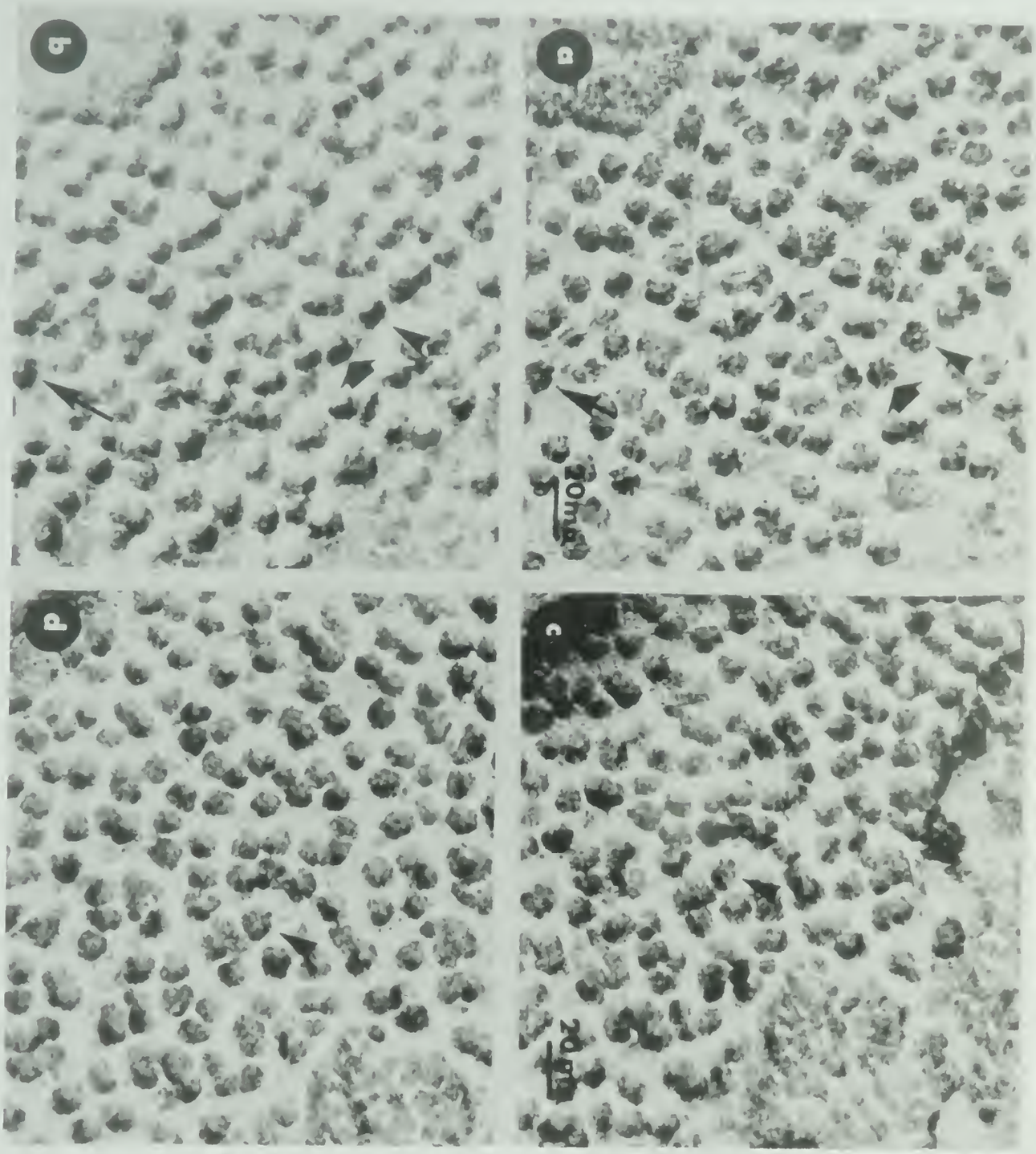
a
b
c
d
20mμ

is photographed at different angles and the resulting photographs subjected to the Markham's rotation. Figures show that the subunits of a symmetrical hexameric structure appear to approach tetrametric symmetry when viewed at an angle of approximately 30°. This is due to the visual distortion of the depth of the model and partial superimposition of at least some of the subunits. Freeze-fracturing involves uncontrolled cleaving of the frozen material where the fracture plane follows the path of least resistance (Sleytr and Robards, 1982). Consequently the plane of the freeze-fracture replica may vary considerably from place to place. When such a relief is photographed in the electron microscope, different electron optical projections of the structures are produced, since the direction of the electron-beam is the same in all these cases. It is, therefore, possible that the deviations from the hexameric symmetry of the connexons are due to the inclination of the fracture plane at that point relative to the plane of viewing. In order to validate this possibility experimentally, tilting experiments were performed using a goniometer stage. It is obvious from Figs. 11 a-d that the tilting of the connexons at varying angles results in projections with different substructures and dimensions. Yet another important factor which could be responsible for departures from hexameric symmetry of connexons is the plastic deformation (discussed in section 4.3.1.6) of subunits during feeze-fracturing.

Plate 10

Figure 12

a. A typical fractured face of an unfixed uncryoprotected rapid-frozen gap junction. Irregular arrangement of intramembranous particles (connexons) is evident on P (protoplasmic) face. The arrow points at an unusually large particle probably representing two clumped connexons. - E Exoplasmic fractured face. - Bar 30 nm.

b. A representative P-fractured face of an fixed (1/2 h with glutaraldehyde) and rapid-frozen gap junction. Connexons appear to be more closely packed than in Figure 12**a**. Large (within circles) and small (arrows) aggregates of particles are encountered more frequently. Same enlargement as Figure 12**a**.

c. Treated in the same way as the one in Figure 12**b**, but for a prolonged fixation with glutaraldehyde (2 h). Large (within circles) and small (arrows) aggregates of connexons can be observed. - P. E Protoplasmic and exoplasmic fractured faces, respectively. Same magnification as in Fig. 12**a**.

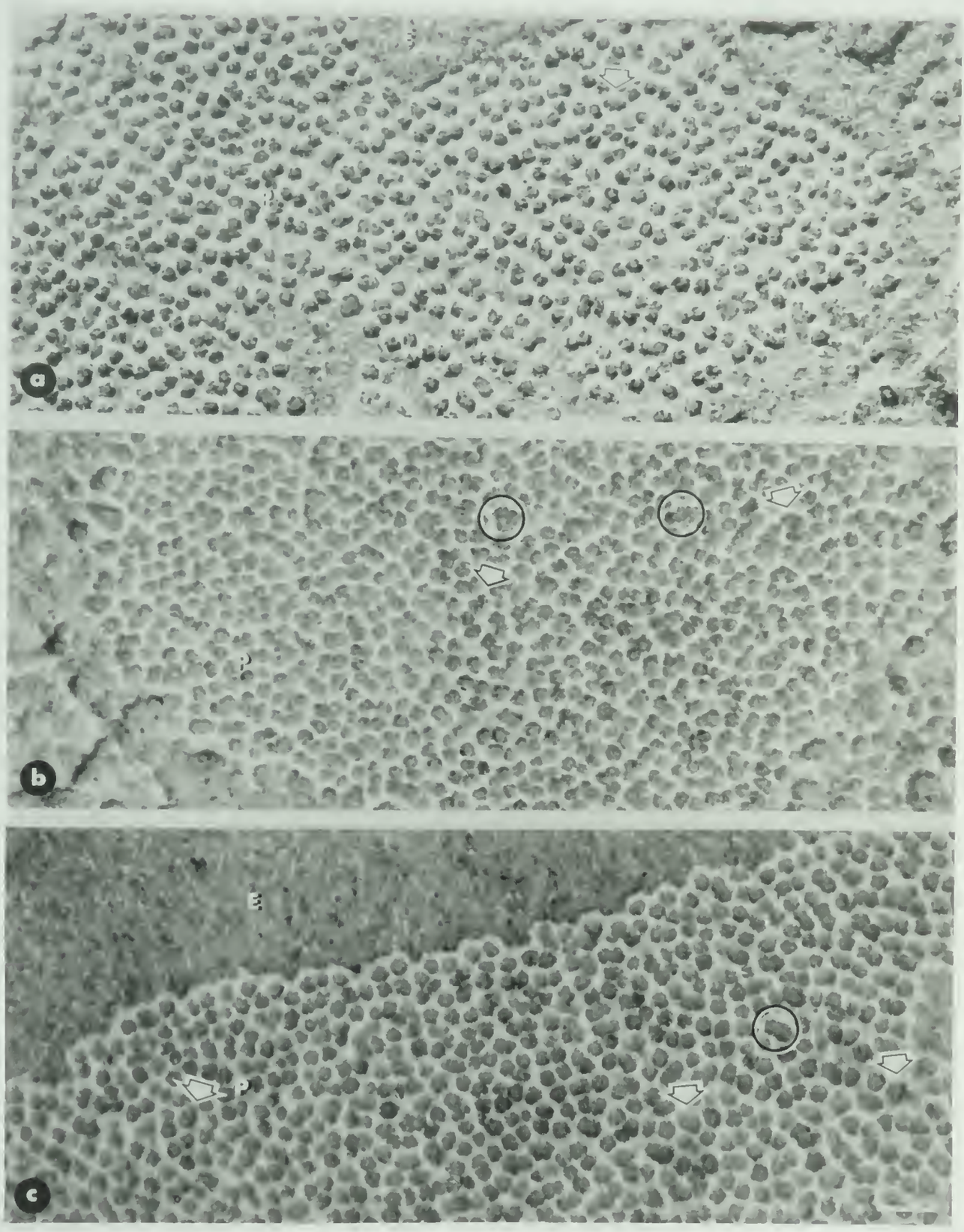
a
b
P
c
E
P

4.3.3 Effect of Fixation with Glutaraldehyde

Fig. 12 a displays a typical freeze-fracture replica of an unfixed uncryoprotected and rapid frozen gap junction. As described in the previous section of this Chapter, the arrangement of connexons on the P face is rather irregular, whereas the E face has the usual rough texture (Bennett and Goodenough, 1978). The fracture faces of the glutaraldehyde fixed and rapid frozen (Fig. 12 b) gap junctions are very similar in appearance to those of unfixed and rapid frozen (Fig. 12 a) ones but for the packing of the conexons which appears to be more "close-packed" in the case of the fixed material. An analysis of the frequency distribution of various interconnexon spacings reveals that the connexons are indeed more closely packed in the fixed preparations (Fig. 13). The average interconnexon spacing in the case of unfixed preparations is 10 $\pm$ 2 nm, and the connexons are arranged at various centre-to-centre spacings ranging from about 5.5 nm to 18.5 nm. However, in the case of fixed preparations (fixed for 1/2 h), the average interconnexon spacing has decreased to 9 $\pm$ 2 nm. As the frequency distribution of interconnexon spacings clearly illustrate (Fig. 13), there is an overall shift towards the smaller spacings upon fixation. Increasing the duration of fixation to 2 hrs. (Fig. 12 c) has no further appreciable effect on the frequency distribution of interconnexon spacing, which remains more or less similar to the one obtained for a specimen fixed for only 1/2 h (Fig. 14). In the case of fixed, glycerinated and conventionally frozen (in liquid Freon 22) and freeze-fractured specimen, the average interconnexons spacing of 9 $\pm$ 2 nm is very

Plate **11**

Figure 13

Frequency distribution of the interconnexon spacings (centre-to-centre) in the unfixed and fixed rapid-frozen gap junctions. A total of 800 spacings were measured on 8 to 10 different gap junctions. In the case of unfixed specimen, the average interconnexon spacing is 10 $\pm$ 2 nm (1% of the total spacings are below 5.4 nm limit and 0.5% are above the 15.5 nm limit. These have not been included in the histogram.) For the specimen fixed for 1/2 h the average interconnexon spacing is 9 $\pm$ 2 nm. (There are 4.3% spacings below 5.5 nm limit and 0.1% higher than 14.5 nm limit.) A distinct shift towards lower spacings is evident upon fixation. Lower limits of groups separated by 1 nm intervals are given.

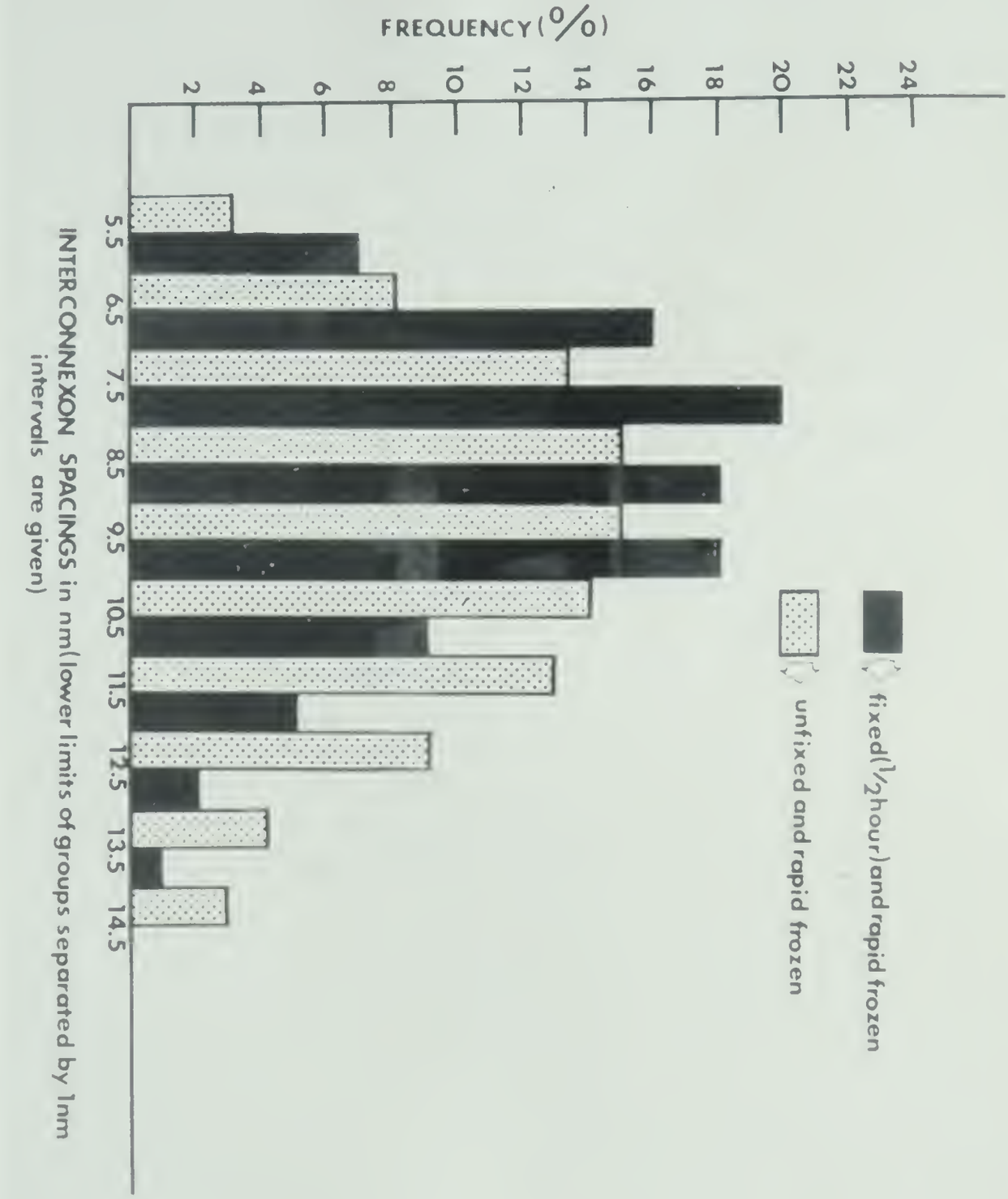
FREQUENCY (%)
2
4
6
8
10
12
14
16
18
20
22
24
5.5
6.5
7.5
8.5
9.5
10.5
11.5
12.5
13.5
14.5
fixed (½ hour) and rapid frozen
unfixed and rapid frozen
INTERCONNEXON SPACINGS in nm (lower limits of groups separated by 1nm intervals are given)

Plate 12

Figure 14

A frequency distribution of the interconnexon spacings (centre-to-centre) in the fixed (for 2 h) and rapid-frozen gap junctions. Total of 800 spacings measured on 6 different gap junctions. The average interconnexon spacing is 9 $\pm$ 2 nm. (2.5% spacing are below 5.5 nm limit and 0.9% spacings are greater than 14.5 nm.) Lower limits of groups separated by 1 nm intervals are given.

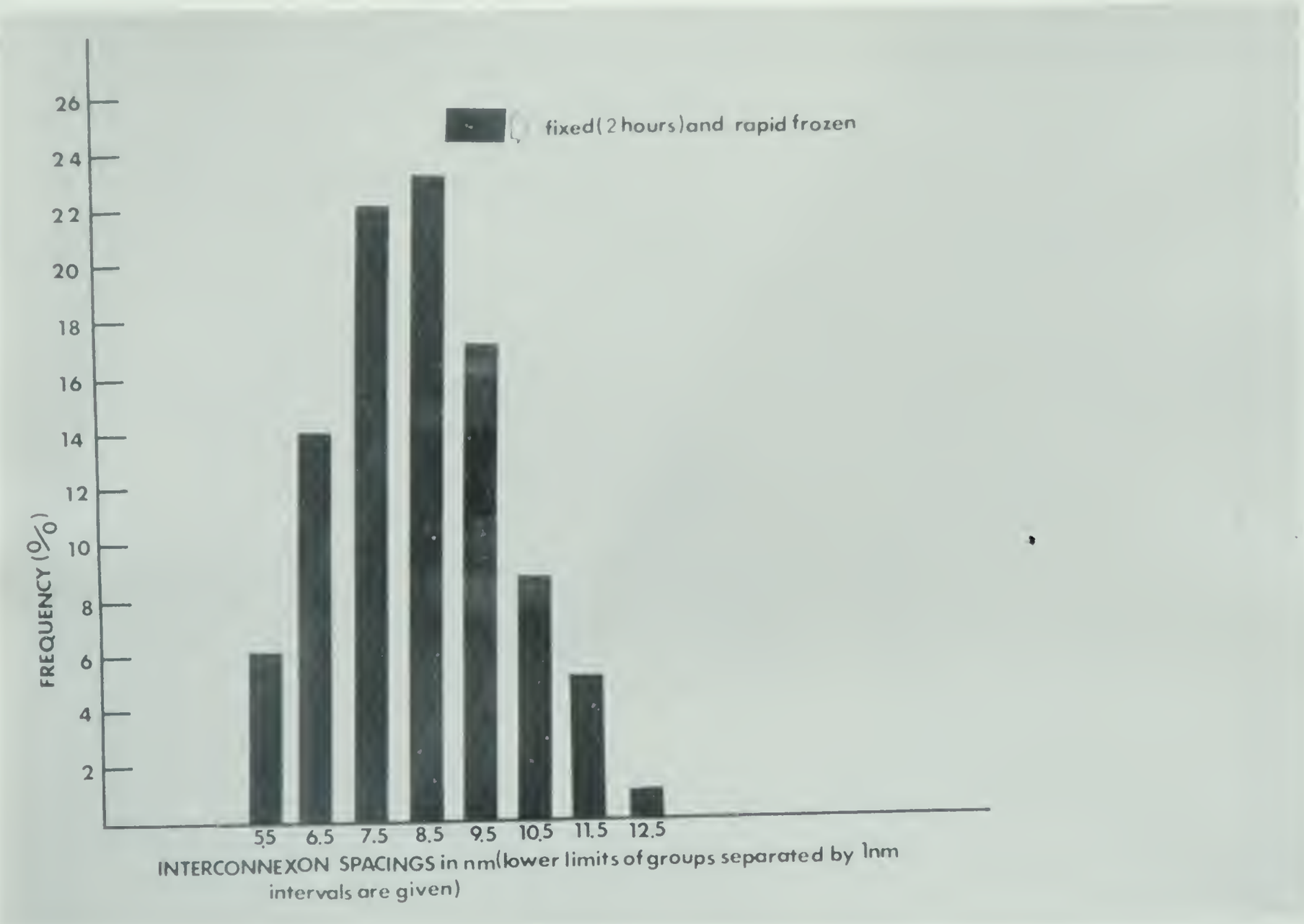
fixed(2 hours)and rapid frozen
FREQUENCY (%)
26
24
22
20
18
16
14
12
10
8
6
4
2
5.5
6.5
7.5
8.5
9.5
10.5
11.5
12.5
INTERCONNEXON SPACINGS in nm(lower limits of groups separated by 1nm intervals are given)

close to that of the fixed and rapid frozen specimen. This effect of glutaraldehyde fixation is present regardless of the buffers employed to prepare glutaraldehyde solutions. Results obtained with 2.5% glutaraldehyde in phosphate buffer (pH 7.4) are similar to those obtained with 2.5% glutaraldehyde in cacodylate buffer (pH 7.4).

Occasionally, rather large particles are observed on the P-fracture faces of gap junctions which could be easily made up of the aggregates of two or more connexons. Some intermediate structures are also observed where two or more connexons are rather closely lumped together. This has given rise to some of the very small spacings displayed in the histogram of Figures (13) and (14). These features are rarely observed in the unidirectionally shadowed preparations. Radially symmetrical contrast brought about by the rotary shadowing reveals these features clearly.

4.4 Discussion

4.4.1 Structure of the Connexons

It is evident from the results reported above that the connexons are hexamers of subunits *in situ*. This *in situ* structural organization of the connexons is in agreement with the results derived from X-ray diffraction (Caspar et al., 1977; Makowski et al., 1977) and low-dose three-dimensional reconstruction studies on isolated liver gap junctions (Unwin and Zampighi, 1980). The hexagonal packing of the connexons displayed in isolated junctions is also suggestive of an internal six-fold symmetry. Apparent departures from the six-fold symmetry (encountered in the freeze-fracture replicas) are caused by

irregular fracture plane and/or plastic deformation. In this connection it is instructive to note that connexons in crayfish neurons are known to have six sub-units (Peracchia, 1973a; Peracchia, 1973b; Peracchia, 1980) while those in the supporting cells in accousticovestibular receptors in goldfish and guinea pig have 5 to 6 subunits (Hama and Saito, 1977). Also, based on orthopgonal and rhombic packing of connexons in isolated junctions from calf eye lens, the presence of only 4 subunits in the connexon has been suggested (Peracchia and Peracchia, 1980). Recently (Zampighi et al., 1981), structural organization of isolated bovine lens fiber junctions has been investigated by electron microscopy and X-ray diffraction. It appears as if each junctional unit is a tetramer of subunits arranged on a square lattice with a center-to-center spacing of 6.6 nm. These junctions are structurally and chemically different from the gap junctions and presumably represent a new class of intercellular contacts. Their amino acid composition is different from that of hepatic junctions (Nicholson et al., 1980) and peptide-map studies have failed to reveal any homology between the liver and lens junctions (Hertzberg, 1980). This conclusion is further substantiated by the observation that the antibodies to the lens junction polypeptide do not cross-react with the liver gap junction polypeptide (Hertzberg, 1980).

It has been claimed that the changes in the distribution of intramembranous particles representing connexons are representative of different functional states of gap junctions. Several authors (Peracchia, 1977, 1978; Baldwin, 1979; Dahl and Isenberg, 1980; Peracchia and Peracchia 1980a, 1980b) have observed that the connexons

are induced to back to form nearly hexagoal arrays upon treatments that physiologically uncouple the cells. Such treatments include low pH and/or high intracellular concentration of Ca^{2+}, metabolic inhibition, anorexia and injury (Lowenstein, 1981). The relationship between the close-backing and uncoupling is not clear in structural terms. The connexons in rapid frozen gap junctions appear to be randomly arrayed. Furthermore, the connexons in the P-fracture face display a central depression that corresponds to the opening of the axial hydrophilic channel near their apical ends. Since these features are also observed in glutaraldehyde-fixed gap junctions which are supposed to be in an uncoupled state, the channel-closing structure is evidently not localized in these regions. Very recently, Hirokawa and Heuser (1982) have visualized the apposed outside surfaces of gap junctions split with hypertonic saline solutions. These surfaces display uniform 8-9 nm particles with central pores or slits, regardless of the functional states of gap junctions. Therefore it is apparent that the channel closing mechanism is not localized in this region too. These authors conclude that the channel closing mechanism is most likely situated at or near the cytoplasmic side, because the pores cannot be seen on the insides of uncoupled junctional membranes. This is in concordance with the model proposed by Unwin and Zampighi (1980) for the three-dimensional structure of gap junction. However, these observations cannot be reconciled with a model proposed by Makowski et al. (1977) on the basis of X-ray diffraction studies which localizes the channel-closing mechanism at the apices of connexons in the extracellular space.

Gap junctions in the heart of the tunicate, Ciona, have been observed in functionally coupled and uncoupled states by employing rapid freezing and freeze-fracturing (Hanna et al., 1981). Rotary shadowed replicas reveal particles that are inhomogenous with respect to size and shape. They appear to be square, pentagonal or hexagonal in shape. However the square and pentagonal forms are predominant. Notwithstanding the noise due to platinum grains (because platinum presumably "decorates" rather than "coats" at this resolution, Slayter, 1976) and plastic deformation, a uniformly hexagonal structure of connexons has been questioned by these authors.

It is evident that radially symmetrical contrast through rotary shadowing of freeze-fracture replicas (Margaritis et al., 1977) consistently permits the direct visualization of the substructure in the connexons. As stated previously, such a substructure has so far only infrequently been visualized by other techniques. Furthermore, X-ray diffraction and low-dose three-dimensional reconstruction studies can be applied only to isolated gap junctions. Such isolation procedures are known to uncouple the junctional channels (Bennett and Goodenough, 1978). Therefore, the method employed here consistently allows a direct observation of the connexon substructure in their native state in situ without any chemical treatment. Such an approach in conjunction with physiological experiments should be valuable in enhancing our understanding of the functioning of the gap junctions.

4.4.2 Structural Correlates of Glutaraldehyde Induced Uncoupling

It is obvious from the observation reported in this Chapter that the glutaraldehyde fixation causes a condensation of the lattice of connexons in the mouse liver gap junctions. The extent of condensation does not appear to increase noticeably with the increase in the duration of fixation. Even in fixed, glycerinated tissues which were frozen in liquid Freon 22, the average interconnexon spacing remains approximately the same as in the case of fixed rapidly frozen ones. It appears that the glutaraldehyde-induced contraction of the gap junction lattice is achieved within a short period of fixation and no further contraction is discernible upon extending fixation.

Available experimental evidence suggests that the uncoupling treatments, such as an increase in the concentration of intracellular free Ca^{2+} and/or H^{+}, trigger the connexons to pack more closely in the gap junctions (Bennett and Goodenough, 1978). It has been suggested that a rise in the concentration of free intracellular Ca^{2+} and/or H^{+} induces a conformational change in the connexons. This change obliterates the channel and increases the affinity between the individual connexons, thus causing them to pack more closely in nearly hexagonal arrays (Peracchia, 1980). Furthermore, it has been demonstrated electrophysiologically that the fixation with glutaraldehyde rapidly uncouples the cells (Bennett et al., 1972). Pronounced uncoupling was noticed after 30 seconds of fixation and within a few minutes a stable high level of uncoupling was attained. These effects remained unchanged regardless of whether the glutaraldehyde solution

was prepared in cacodylate buffer or phosphate buffer. Similar observations have also been made on the crayfish septate axons (Politoff and Pappas, 1972). The sensitivity of gap junctional conductance and its pH and voltage dependence to glutaraldehyde fixation have been reported recently and it has been suggested that glutaraldehyde changes the junctional channel, thereby reducing its conductance, and induces alterations at the site(s) at which protons act to gate the channel conductance (Spray et al., 1981).

Glutaraldehyde is known to alter the transport properties of other channels as well. In the case of nervous transmission, fixation with cross-linking aldehydes (and notably with glutaraldehyde) reduces the amplitude and increases the width of the action potential (Shrager et al., 1969). It has been speculated that aldehyde fixation induces a conformational change in the membrane protein involved in the excitation. A simple, passive blocking of the channel was considered to be unlikely. Glutaraldehyde has also been reported to affect the Na and K currents in squid axon by reducing the peak inward current of Na, partially or completely inhibiting the Na-inactivation and reducing the K current (Horn et al., 1978).

The effect of glutaraldehyde fixation on the frequency dependent dielectric constants and loss factors and DC conductivities of collagen has also been investigated (Milch and Frisco, 1965). Glutaraldehyde treatment results in a considerable decrease in the dielectric constant, loss factor and conductivity of collagen in comparison to the untreated controls. It appears that the dipoles in collagen that are normally free to orient in the applied alternating electric field are

"frozen" in by the chemical cross-linking reagents such as glutaraldehyde. In all these cases described above, glutaraldehyde (by virtue of its cross-linking properties) causes extensive conformational change upon fixation. This is further supported by the observations that the glutaraldehyde fixation results in the loss of secondary α-helical structures of membrane proteins. As monitored by the circular dichroism spectra, the glutaraldehyde fixation reduces the α-helical content of the red blood cell membranes by as much as 22% (Lennard and Singer, 1968). Alterations induced upon fixation with glutaraldehyde have been studied in myelin by X-ray diffraction and electron microscopy. Electron density profiles computed from X-ray diffraction patterns display marked alterations in both packing and molecular structure of myelin membranes upon fixation with aldehydes. At the cytoplasmic boundaries, membranes become more closely apposed with an enhanced electron density whereas the membranes at the external boundries manifest increased separation (Kirschner and Hollingshead, 1980). Based upon the known strong cross-linking and denaturing properties of glutaraldehyde, it appears likely that the fixative induced contraction of the lattice of connexons (and uncoupling) is a result of some conformational changes in the junctional proteins. Probably the uncoupling induced upon fixation with glutaraldehyde follows a different mechanism in comparison to the uncoupling action of the classical uncouplers such as the concentrations of free intracellular Ca^{2+} and/or H^{+} ions (Peracchia, 1980). Treatment of mouse liver with such functional uncouplers prior to fixation causes the aggregation of connexons into almost crystalline two-dimensional arrays (Raviola et al., 1980). It has been suggested

that glutaraldehyde fixation interferes with the propensity of the uncoupled junctions to crystallize slowly into two-dimensional crystals (Raviola et al., 1980). These authors have frozen the mouse livers at 4°K by employing a rapid-freezing technique involving the use of liquid helium (Heuser et al., 1979). They observed that the gap junctions in the liver are "scarcely affected" by fixatives. No difference has been reported between the fixed and unfixed eye lens gap junctions (Peracchia and Peracchia, 1980). Therefore, it appears that the sensitivity of gap junction structure to fixation with glutaraldehyde varies considerably from tissue to tissue. The difference between the sensitivities of liver and eye lens gap junctions is expected because these two gap junctions differ structurally as evidenced by some preliminary observations on the molecular packing and partial amino-acid sequence (Nicholson et al., 1980; Peracchia and Peracchia, 1980; Robertson et al., 1981).

5. CONCLUSIONS

Although the specific molecular details of the structure and mechanism operative in the process of intercellular communication are as yet not resolved, the accumulated evidence indicates that the gap junctions are almost ubiquitous plasma membrane organelles in organized animal tissues specifically designed for intercellular communication. These gap junctions provide the hydrophilic channels to allow ions and small molecules to diffuse from cell to cell and thus establish a physiological continuum.

With an overall objective to study their high resolution three-dimensional structure, a method has been developed to isolate the gap junctions from mouse liver in which proteolysis is minimized and the use of urea has been eliminated (urea is known to denature proteins). The plasma membranes are solubilized by an anionic detergent, n-dodecanoyl sarcosine, in combination with non-ionic polyoxyethylene alcohol detergents (Brij 35 and 58) and a non-ionic polyoxyethylene ether detergent (W-1). Purified gap junctions are obtained by centrifugation in a sucrose step-gradient containing 1-O-n-octyl-α-(D) glucopyranoside. The gap junctions thus obtained are comprised of single polypeptide of a 26,000 Mr as determined by the SDS-PAGE. The connexons in these gap junctions are organized on a hexagonal lattice of lattice constant 7.6-8.4 nm as revealed by electron microscopy, optical diffraction and X-ray diffraction studies.

The potential of these purified gap junctions for the elucidation of high-resolution structure by employing low-dose

Fourier transform electron imaging and diffraction methods (Unwin and Henderson, 1975) is yet to be explored. Since the isolated procedure provides high yields of gap junctions, attempts can be made to recrystallize connexons into well-ordered, extended two-dimensional crystals suitable for high resolution structural analysis. Such crystals when available, would overcome the problem of inherent short range disorder and/or high degree of mosaicity in the conventional preparations of gap jucntions, that has limited the currently attainable resolution to approximately 1.8 nm (Zampighi and Unwin, 1979). In addition, the elucidation of the structure of connexons in various crystal forms would not only provide information on how molecules interact in different environment which is of immediate relevance to model building (Englemann et al., 1980), but can also be employed in the determination of accurate high-resolution three-dimensional phases by the molecular replacement method (Rossmann and Henderson, 1982). Such an approach has already paved way to the successful determination of the projected structure of the purple membrane (in Halobacterium halobium) at 0.33 nm resolution. The presence of the hydrophilic channel in the connexons can be readily distinguished by employing neutron scattering in conjunction with isomorphous contrast variation using H_2O/D_2O exchange techniques (Stuhrmann, 1982).

Gap junctions are considered to be dynamic structures susceptible to perturbations in the homeostasis. It has been claimed that the isolation procedures uncouple the gap junctions as they involve the disruption of tissues and cells (Peracchia, 1980); hence it has been argued that the structure of gap junction determined by electron

microscopy and X-ray diffraction on the isolated gap junction fractions may not represent an *in situ* structure (Peracchia, 1980). Therefore, it was considered desirable to study the *in situ* structure of the gap junctions. Such a study has been made by employing rapid freezing, freeze-etching and rotary shadowing in conjunction with Markham's method (Markham et al., 1963) for rotational integration. The connexons have emerged as having an hexameric sub-unit organization enclosing a region corresponding to a part of the putative axial hydrophilic channel. Deviations from hexameric symmetry are likely to be due to plastic deformation and/or an uneven fracture plane. It is obvious that the radially symmetrical contrast produced by rotary shadowing in conjunction with rapid freezing is capable of resolving individual sub-units of connexons and the putative hydrophilic channel. Such an approach in conjunction with physiological experiments should find applications in providing structural correlates of the gap junctional channels *in situ*.

In the past, structural changes in the gap junctions, induced upon uncoupling treatments, have been studied by freeze-fracturing technique involving chemical fixation with glutaraldehyde and cryoprotective treatment with glycerol. However, fixation with glutaraldehyde is known to readily abolish the coupling as first pointed out by electrophysiologists. Therefore, the structural changes induced upon fixation with glutaraldehyde have been elaborated by employing rapid freezing without prior cryoprotection. It appears as if fixation with glutaraldehyde induces the connexons to pack tightly, as the average interconnexon spacing decreases from 10 nm to 9 nm. In light of

the well-known cross-linking and denaturing properties of glutaraldehyde-fixation induced uncoupling presumably follows a different path than functional, reversible uncoupling action of classical uncouplers, such as the concentrations of free Ca^{2+} and/or H^{+} ions in the cytoplasm.

In summary, a new procedure that aims at minimizing proteolysis has been developed to isolate gap junctions from mouse liver. This method involves use of some of the detergents hitherto not used for the isolation of gap junctions. The gap junctions thus obtained are comprised of a single polypeptide of 26,000 Mr as established by SDS-PAGE. Packing of connexons in these junctions has been determined by electron microscopy (involving optical diffraction) and X-ray diffraction. The connexons are arranged on a hexagonal lattice with a lattice constant of approximately 7.6-8.4 nm. The hexameric sub-unit structure of these connexons in situ has been confirmed by rapid freezing coupled with freeze-fracturing, rotary shadowing and Markham's rotational filtering technique for contrast enhancement. These sub-units line-up to enclose the putative aqueous channel. The structural correlates of glutaraldehyde-induced uncoupling have been studied and such a fixation results in the close-packing of connexons.

6. BIBLIOGRAPHY

Agard, D.A. and Stroud, R.M. (1982). Linking regions between helices in bacteriorhodopsin revealed. Biophys. J. 37, 589.

Arnow, R.H. (1963). Statistical mechanics of micelles. J. Phys. Chem. 67, 556.

Astbury, W.T. (1933). Some problems in the X-ray analysis of the structure of animal hairs and protein fibres. Trans. Faraday Soc. 29, 193.

Azarina, R., Michalke, W. and Lowenstein, W.R. (1972). Intercellular communication and tissue growth. J. Membr. Biol. 10, 247.

Bald, W.B. and Robards, A.W. (1978). A device for rapid freezing of biological specimens under precisely controlled and reproducible conditions. J. Microsc. 112, 3.

Baldwin, K.M. (1979). Cardiac gap junction configuration after an uncoupling treatment as a function of time. J. Cell Biol. 82, 66.

Baker, T.S., Caspar, D.L.D., Hollingshead, C.J. and Goodenough, D.A. (1983). Gap junction structures, IV. Asymmetric features revealed by low-irradiation microscopy. J. Cell Biol. 96, 204.

Barrantes, F.J. (1975). The nicotinic cholinergic receptor: different compositions evidenced by statistical analysis. Biochem. Biophys. Res. Commun. 62, 407.

Benedetti, E.L. and Emmelot, P. (1968). Hexagonal arrays of subunits in tight junctions separated from isolated rat liver plasma membranes. J. Cell Biol. 38, 15.

Bennett, M.V.L. (1977). In "Handbook of Physiology" (E.R. Kandel, ed.), I. The Nervous System, Sect. I: Cellular Biology of Neurons, pp. 357. Williams and Wilikins, Baltimore, Maryland.

Bennett, M.V.L., Spira, M.E. and Pappas, G.D. (1972). Properties of electrotonic junctions between embryonic cells of Fundulus. Dev. Biol. 29, 419.

Bennett, M.V.L. and Goodenough, D.A. (1978). Neurosci. Res. Prog. Bull. 16, 373.

Bernal, J.D. (1964). The structure of liquids. Proc. Roy. Soc. (London) A 280, 299.

Blaurock, A.E. (1975). Bacteriorhodopsin: a transmembrane pump containing -helix. J. Mol. Biol., 93, 139.

Blodgett, K.B. (1935). Films built by depositing successive monomolecular layers on a solid surface. J. Am. Chem. Soc. 57, 1007.

Blundell, T.L. and Johnson, L.N. (1976). Protein Crystallography. Academic Press, New York.

Born, M. and Wolf, E. (1975). Principles of Optics (fifth ed.). Pergamon Press, Oxford.

Branton, D. (1966). Fracture faces of frozen membranes, Proc. Natl. Acad. Sci. USA, 55, 1048.

Branton, D. (1971). Freeze-etching studies of membrane structure. Phil. Trans. Roy. Soc. London (series B), 261, 133.

Branton, D. and Park, R.B. (1967). Subunits in chloroplast lamellae. J. Ultrastruct. Res. 19, 283.

Branton, D., Bullivant, S., Gilula, N.B., Karnovsky, M.J., Moor, H., Muhlethaler, K., Northcote, D.H., Packer, L., Satir, B., Satir, P., Speth, V., Staehlin, L.A., Steere, R.L. and Weinstein, R.S. (1975). Freeze-etching nomenclature, Science, 190, 54.

Brestscher, M.S. and Ratt, M.C. (1975). Mammalian plasma membranes. Nature, 258, 43.

Bruggeller and Mayer (1980). Complete vitrification in pure liquid water and dilute aqueous solutions. Nature, 288, 569.

Bruggeller and Mayer (1982). Vitrification of pure liquid water by high pressure jet freezing. Nature, 298, 715.

Brunette, D.M., and Till, J.E. (1971). A rapid method for the isolation of L-cell surface membranes using an aqueous two-phase polymer system. J. Membr. Biol. 5, 215.

Buerger, M.J. (1960). Crystal Structure Analysis, Robert E. Krieger Publishing Comp. New York, 1980.

Carslaw, H.S. and Jaeger, J.C. (1974). Conduction of Heat in Solids, Clarendon Press, Oxford.

Caspar, D.L.D., Goodenough, D.A., Makowski, L. and Phillips, W.C. (1977). Gap junction structures, I. correlated electron microscopy and X-ray diffraction. J. Cell Biol. 74, 605.

Chalcroft, J.P. and Bullivant, S. (1970). An interpretation of liver cell membrane and junction structure based on observation of freeze-fractured replicals of both sides of the fracture. J. Cell Biol. 47, 49.

Chen, R., Kramer, C., Schimidmayr, W. and Henning. U. (1979). Primary structure of major outer membrane protein I or Escheria coli B/r. Proc Naltl. Acad. Sci. USA, 76, 5014.

Chou, P.Y., and Fasman, A.D. (1978). Ann. Rev. Biochem., 47, 251.

Clark, A.W. and Branton, D. (1968). Fracture faces in frozen outer segments from guinea pig retina. Z. Zellforsch. Mikrosk. Anat., 91, 586.

Cole, K.S. (1968). Membranes Ions an Impulses, University of California Press, Berkeley.

Collander, R. (1937). The permeability of plant protoplasts to non-electrolytes. Trans. Faraday Soc. 33, 958.

Conti, F., DeFelice, L.J., and Wanke, E. (1975). Potassium and sodium ion current noise in the membrane of the giant squid axn. J. Physiol. London 248, 45.

Costello, M.J. (1980). Ultrarapid freezing of thin biological samples, Scan. Electr. Microsc. II, 361.

Costello, M.J. and Corless, J.M. (1978). The direct measurement of temperature changes within freeze-fracture specimens during rapid quenching in liquid coolants. J. Microsc. 112, 17.

Costello, M.J., Fetter, R. and Hochli, M. (1982). Simple procedures for evaluating the cryofixation of biological samples. J. Microsc. 125, 125.

Cowie, J.M.G. (1973). Polymers: Chemistry and Physics of Modern Materials. International Textbook Company, Great Britain.

Cowley, J.M. (1981). Diffraction Physics (2nd Edition). North-Holland Publishing Company, New York.

Crick, F.H.C. (1953). The packing of -helices: simple coiled-coils Acta. Cryst. 6, 689.

Crick, F.H.C. (1970). Diffusion in Embryogenesis, Nature 225, 420.

Culvenor, J.C. and Evans, W.H. (1977). Preparation of hepatic gap (communicating) junctions. Biochem. J. 168, 475.

Dahl, G. and Isenberg, G. (1980). Decoupling of heart muscle cells: correlation with increased cytoplasmic calcium activity and with changes of nexus ultrastructure. J. Membr. Biol. 53, 63.

Dawson, H. and Danielli, J.F. (1943). The permeability of natural membranes (2nd ed. 1952): Cambridge, University Press.

Deamer, D.W. and Branton, D. (1967). Fracture planes in an ice-bilayer model membrane system. Science 158, 655.

Deamer, D.W., Leonard, R., Tardieu, A. and Branton, D. (1970). Lameller and hexagonal lipid phases visualized by freeze-etching. Biochim. Biophys. Acta. 219, 47.

DeRosier, D. and Klug, A. (1968). Reconstruction of three-dimensional structures from electron micrographs, Nature, 217, 130.

Dorling, P.R. and LePage, R.N. (1973). A rapid high yield method for the preparation of rat liver cell plasma membranes. Biochim. Biophys. Acta. 318, 33.

Duguid, J.R. and Revel, J.P. (1975). The protein component of the gap junction. Cold spring Harbor Symp. Quant. Biol. 40, 45.

Dunia, I., Senghosh, C., Benedetti, E.L. Zweers, A. and Bloemendel, H. (1974). Isolation and protein pattern of eye lens fiber junctions. FEBS. Lett. 45, 139.

Dunitz, I.D. (1979). X-ray Analysis and the Structure of Organic Molecules, Cornell University Press, Ithaca.

Dunlop, W.F. and Robards, A.W. (1972). Some artifacts of the freeze-etching technique. J. Ultrastruct. Res. 40, 391.

Dunlop, W.F. and Robards, A.W. (1973). Ultrastructural study of poly-B-hydroxybutyrate granules from Bacillus cereus. F. Bacl. 114, 1271.

Earnshaw, W.C., Goldberg, E.B. and Crowther, R.A. (1979). Phage T4 tail fibre structure. J. Mol. Biol. 132, 101.

Edwards, H.H., Mueller, T.J. and Morrison, M. (1979). Distribuion of transmembrane polypeptides in freeze-fracture. Science 203, 1343.

Ehrhart, J.C. and Chauveau, J. (1977). The protein component of mouse hepatocyte gap junctions. FEBS. Lett. 78, 205.

Emmelot, P., Bos, C.J., Van Hoeven, R.P. and Van Blitterswijk, W.J. (1974). Isolation of plasma membranes from rat and mouse livers and hepatomas. Meth. Enzymol. XXXI (pt. A), 75.

Engleman, D.A., Henderson, R., MacLachlan, A.D. and Wallace, B.A. (1980). Proc. Natt. Acad. Scr. USA, 77, 2023.

Evans, W.H. (1980). Communication between cells. Nature 283, 521.

Evans, W.H., and Gurd, J.W., (1972). Preparation and properties of nexus and lipid enriched vesicles from mouse liver plasma membranes. Biochem. J., 128, 691.

Fallon, R.F. and Goodenough, D.A. (1981). Five-hour half-life of a mouse liver gap-junction protein. J. Cell Biol. 90, 521.

Ferguson, K.A. (1964). Starch gell electrophoresis - application to the classification of pitutary proteins and polypeptides. Metab. Clin. Exp. 13, 985.

Finbow, M., Yancey, S.B., Johnson, R. and Revel, J.P. (1980). Independent lines of evidence suggesting a major gap junctional protein with a molecular weight of 26,000. Proc. Natt. Acad. Sci. USA, 77, 970.

Finch, J.T. (1975). Electron microscopy of proteins in The Proteins (third ed.), Vol. I (H. Neurath and R.L. Hill eds.), Academic Press, New York, 413.

Fish, W.W., Reynold, J.A. and Tanford, C. (1970). Gel chromatography of proteins in denaturing solvents. J. Biol. Chem. 245, 5166.

Flagg-Newton, J.L., Simpson, I. and Lowenstein (1979). Permeability of cell-to-cell membrane channels in mammalian cell jucntion. Science 205, 404.

Fleisher, S., Fleisher, B. and Stoeckenius, W. (1967). Fine structure of lipid depleted mitochondria. J. Cell Biol. 32, 193.

Folch Pi, J. and Stoffyn, P.J. (1972). Proteolipids from membrane systems, Ann. N.Y. Acad. Sci. 195, 86.

Franks, F. (1980). Physical, biochemical and physiological effects of low-temperatures and freezing - their modification by water soluble polymers. Scan. Electr. Microsc. II, 349.

Fraser, R.D.B. and MacRae, T.P. (1973). Conformation in Fibrous Proteins Academic Press, N.Y.

Furshpan, E.J. and Potter, D.D. (1959). Transmission at the giant motor synapses of crayfish. J. Physiol. London, 145, 289.

Gabler, R. (1978). Electrical Interactions in Molecular Biophysics, Academic Press, New York.

Gierer, A. (1981). Some physical, mathematical and evoluationary aspects of biological pattern formation. Phil. Trans. Roy: Soc. Lond. B295, 429.

Gilula, N.B. (1972). Cell junctions of the crayfish hepatopancreas. J. Ultrastruct. Res. 58, 215a.

Gilula, N.B. (1980). Cell-to-cell communication and development in Membrane-Membrane Interactions (Gilula, N.B., ed.), Reven Press, New York.

Gilula, N.B., Reeves, O.R., and Steinbach, A. (1972). Cell-to-cell communication and metabolic cooperation. Nature 235, 262.

Gilula, N.B., Epstein, M.L. and Beers, W.H., (1978). Cell-to-cell communication and cumulus-oocyte complex. J. Cell Biol. 78, 58.

Goodenough, D.A. (1974). Bulk isolation of mouse hepatocyte gap junctions. Characterization of principal protein, connexin. J. Cell Biol. 61, 557.

Goodenough, D.A. (1975). Methods for the isolation and structural characterization of hepatocyte gap junctions. Methods Membr. Biol. III, 51.

Goodenough, D.A. (1975). The structure and permeability of isolated heptocyte gap junctions. Cold Spring Harbor Symp. Quant. Biol. 40, 37.

Goodenough, D.A. (1976). In vitro formation of gap junctional vesicles. J. Cell Biol. 68, 220.

Goodenough, D.A. and Revel, J.P. (1970). A fine structural analysis of intercellular junctions in mouse liver, J. Cell Biol. 45, 272.

Goodenough, D.A. and Stoeckenius, W. (1972). The isolation of mouse hepatocyte gap junctions, preliminary chemical characterization and X-ray diffraction. J. Cell Biol. 54, 646.

Griffin, W.C. (1949). J. Soc. Cosmet. Chem. 1, 311, cited by Helenius and Simons (1975).

Gryns, G. (1896). Dflugers Arch. 63, 86, cited by Peracchia (1980).

Guiner, A. (1963). X-ray Diffraction. W.H. Freeman and Company Publishers, San Fransisco, Calif.

Hama, K. and Saito, K. (1977). Gap junctions between the supporting cells in some accoustico-vestibular receptors. J. Neurocytol. 6, 1.

Hanna, R.B., Rees, T.S., Ornberg, R.L., Spray, D.C. and Bennett, M.V.L. (1981). Fresh frozen gap junctions; resolution of structural detail in coupled and uncoupled state. J. Cell Biol. 91, 125a.

Haydon, D.A. and Taylor, J. (1963). The stability and properties of bimolecular leaflets in aqueous solutions. J. Theoret. Biol. 4, 281.

Hayward, S. and Stroud, R.M. (1981). Projected structure of purple membrane at 3.7A, J. Mol. Biol. 151, 491.

Hedin, S.G. (1897). Pflugers Arch. 68, 229. Referred by Peracchia (1980).

Helenius, A. and Simons, K. (1975). Solubilization of membranes by detergents. Biochim. Biophys. Acta. 415, 29.

Henderson, D., Eibl, H., and Weber, K. (1979). Structure and biochemistry of mouse hepatocyte gap junctions. J. Mol. Biol. 132, 193.

Henderson, R. and Unwin, P.N.T. (1975). Three dimensional model of purple membrane obtained by electron microscopy. Nature 275, 28.

Hendrick, J.L. and Smith, A.J. (1968). Size and charge isomer separation and estimation of molecular weights of proteins by disc gel electrophoresis. Arch. Biochem. Biophys. 126, 155.

Hermann, R.B. (1972). Theory of hydrophobic bonding, II. The correlation of hydrocarbon solubility in water with solvent-cavity surface area. J. Phys. Chem. 76, 2754.

Hertzberg, E.L. (1980). Biochemical and immunological approaches to the study of gap junctional communication. In Vitro, 16, 1057.

Hertzberg, E.L. and Gilula, N.B. (1979). Isolation and characterization of gap junctions from rat liver. J. Biol. Chem. 254, 2138.

Heuser, J.E., Reese, T.S., Dennis, M.J., Jan, L. and Evans, L. (1979). Synaptic vesicle exocytosis captured by quick-freezing and correlated with quantal transmitter release. J. Cell Biol. 81, 275.

Hirokawa, N. and Heuser, J. (1982). The inside and outside of gap-junction membranes visualized by deep etching. Cell, 30, 395.

Hober, R. (1936). The permeability of red blood corpuscles to organic ions. J. Cell Comp. Physiol. 7, 367.

Hooper, M.L., and Subak-Sharpe, J.H. (1981). Metabolic cooperation between cells. Int. Rev. Cytol. 69, 45.

Horn, R., Brodwick, M.S., Eaton, D.C. (1978). Effect of protein cross-linking reagents in membrane current in squid axon. Biophys. J. 21, 429.

Hosemann, R. and Bagchi, S.N. (1962). Direct Analysis of Diffraction by Matter, North-Holland Publishing Company, Amsterdam.

Jacobs, M.H. (1924). Am. J. Physiol. 68, 134. Cited by Peracchia (1980).

Jacobs, M.H. (1935). Diffusion processes, Ergeb. Biol., 12, 1.

James, R. and Branton, D. (1971). The correlation between the saturation of membrane fatty acids and the presence of membrane fracture faces after osmium fixation. Biochim. Biophys. Acta. 233, 504.

James, R.W. (1965). The Optical Principles of the Diffraction of X-rays, G. Bell and Sons Limited, London.

Jost, M. (1965). Die Ultrastruktur von Oscillatoria rubescens, D.C. Arch. Microbiol., 50, 211.

Kanno, Y. and Lowenstein, W.R. (1964). Intercellular diffusion Science 143, 959.

Kanno, Y. and Lowenstein, W.R. (1966). Cell-to-cell passage of large molecules. Nature London, 212, 629.

Kauzmann, W. (1959). Some factors in the interpretation of protein denaturation. Adv. Prot. Chem., 14, 1.

Kennedy, S.J. (1978). Structures of membrane proteins. J. Membr. Biol. 42, 265.

Kirschner, D.A. and Hollingshead, C.J. (1980). Processing for electron microscopy alters membrane structure and packing in myelin. J. Ultrastruct. Res. 73, 211.

Kolodny, G.M. (1972). Fed. Proc. Fed. Am. Soc. Exp. Biol. 31, A607, cited by Hooper and Subak-Sharpe (1981).

Kuffler, S.W. and Potter, D.D. (1964). Glia in the leech central nervous system: physiological properties and neuron-glia relationships, J. Neurophysiol. 27, 290.

Laemmli, U.K. (1970). Cleavage of structural proteins during the assembly of the head of the bacteriophage T4, Nature, 227, 680.

Langmuir, I. (1917). The constitution and fundamental properties of solids and liquids. II. Liquids, F. Am. Chem. Soc. 39, 848.

Langmuir, I. (1939). Pilgrim trust lecture, molecular layers. Proc. Roy. Soc. (London), A, 170, 1.

Lawrence, T.S., Beers, W.H., and Gilula, N.B. (1978). Transmission of hormonal stimulation by cell-to-cell communication, Nature London, 272, 501.

Lennard, J. and Singer, S.J. (1968). Alteration of the conformation of proteins in red blood cell membranes and in solution by fixatives used in electron microscopy. J. Cell. Biol. 37, 117.

Lepault, J. and Dubochet, J. (1980). Freezing, fracturing and etching artifacts in particulate suspensions. J. Ultrastruct. Res. 72, 223.

Lesko, L., Donlon, M., Marinetti, G.V. and Hare, J.D. (1973). A rapid method for the isolation of rat liver plasma membranes using an aqueous two-phase polymer system. Biochim. Biophys. Acta. 311, 173.

Lipson, H. and Cochran, W. (1968). The determination of Crystal Structures (3rd revised edition). G. Bell and Sons, London.

Loewenstein, W.R. (1966). Permeability of membrane junctions, Ann. N.Y. Acad. Sci. USA, 137, 441.

Loewenstein, W.R. (1979). Junctional Intercellular Communication and the Control of Growth, Biochim. Biophys. Acta. 560, 1.

Loewenstein, W.R. (1981). Junctional Intercellular Communication: The Cell-to-Cell Membrane Channel. Physiological Reviews, 61, 829.

Loewenstein, W.R. and Kanno, Y. (1963). Some electrical properties of a nuclear membrane examined with a microelectrode. J. Gen. Physiol. 46, 1123.

Loewenstein, W.R. and Kanno, Y. (1964). Studies on an epithelial (gland) cell junction. I. Modifications of surface membrane permeability, J. Cell Biol. 22, 565.

Lowry, O.H., Resenbrough, N.J., Farr, A.L. and Randall, R.J. (1951). Protein measurement with the folin phenol reagent. J. Biol. Chem. 193, 265.

Maddy, A.H. and M.J. Dunn (1976). Techniques for the analysis of membrane proteins in Biochemical Analysis of Membranes (Maddy, A.H., ed.), Chapman and Hall London, p. 197-251.

Maizel, J.V. (1971). Polyacrylamide gel electrophoresis of viral proteins, in "Methods in Virology" (K. Maramorosch and H. Koprowski, eds.), Vol. 5, Academic Press, 179.

Makowski, L., Caspar, D.L.D., Phillips, W.C. and Goodenough, D.A. (1977). Gap junction structures. II. analysis of the X-ray diffraction data, J. Cell Biol., 74, 629.

Makowski, L., Caspar, D.L.D., Goodenough, D.A. and Phillips, W.C. (1982). Gap junction structures III. The effect of variations in the isolation procedure. Biophys. J., 37, 189.

Margaritis, L.H., Elgaester, A. and Branton, D. (1977). Rotary replication for freeze-etching, J. Cell Biol., 72, 47.

Markham, R.S., Frey, S. and Hills, G.J. (1963). Methods for the enhancement of image detail and accentuation of structure in electron microscopy, Virology, 20, 88.

McNutt, N. and Weinstein, R.S. (1970). The ultrastructure of the nexus. A correlated thin section and freeze-cleave study. J. Cell Biol., 47, 666.

Medzihradsky, F., Kline, M.H. and Hokin, L.E. (1967). Studies on the characterization of Na^+, K^+ transport ATPase. 1. Solubilization, stabilization and estimation of apparent molecular weight. Arch. Biochem. Biophys. 121, 311.

Milch, R.A., Fresco, L.J. and Szymkowiak, E.A. (1965). Solid state dielectric properties of adehyde treated goatskin collagen, Biorrheology, 3, 9.

Misell, D.L. (1978). Image analysis. Enhancement and Interpretation in Practical Methods in Electron Microscopy (A. Galuert, ed.), Vol. 7, North-Holland Publishing Company, New York.

Moore, H. (1973). Cryotechnology for the analysis of biolgoical material, in: Freeze-etching, techniques and applications, (E.L. Benedetti and P. Favard, eds.), Soc. Fra. Microsc. Elect., Paris, p. 11.

Mueller, M., Fischer, W.M., Schmitt, W.W. and Bachmann, L. (1972). Freeze-etching of cells without cryoprotectants. J. Cell Biol. 53, 116.

Nagelli, C. and Cramer, C. (1855). Pflanzenphysiologische Untersuchungen, 1 Heft. Zurich, F. Schultess.

Neville, D.M. (1960). Isolation of a cell membrane fraction from rat liver. J. Biophys. Biochem. Cytol. 8, 413.

Neville, D.M. (1971). Molecular weight determination of protein-dodecyl sulphate complexes by gel electrophoresis in a discontinuous buffer system. J. Biol. Chem. 246, 6328.

Nicholson, B.J., Hunkapiller, M.W., Hood, L.E. and Revel, J.P. (1980). Partial sequencing of gap junctional protein from rat liver and lens. J. Cell Biol. 97, 200a.

Nicholson, B.J., Hunkapiller, M.W., Grim, L.B., Hood, L.E. and Revel, J.P. (1981). Rat liver gap junction protein: Properties and partial sequence. Proc. Natt. Acad. Sci.: USA, 78, 7594.

Overton, E. (1895). Vjshr. Naturf. Ges. Zurich, 40, 159, Cited by Peracchia (1980).

Overton, E. (1899). Ueber die algemeinen osmotishen Eigenschaften der Zelle, Ihre vermutlichen Ursachen und ihre Bedeutung fur die Physiologie. Vjochr, Naturf. Gex. Zurich. 44, 88.

Park, R.B. and Branton, D. (1966). Freeze-etching of chloroplasts from glutaraldehyde fixed leaves. Brookhaven Symp. Biol. 19, 341.

Pauling, L., Corey, R.B. and Branson, A.R. (1951). The structure of proteins: two hydrogen bonded helical configurations of the polypeptide chain. Proc. Natl. Acad. Sci. USA, 37, 205.

Pauling, L. and Corey, R.B. (1951). Configurations of polypeptide chains with favoured orientation around single bonds: two new β pleated sheets. Proc. Natl. Acad. Sci. USA, 37, 729.

Payton, B.W., Bennett, M.V.L. and Pappas, G.D. (1969). Permeability and structure of junctional membranes at an electrotonic synapse. Science, 166, 1641.

Peracchia, C. (1973 a). Low resistance junctions in crayfish I. Two arrays of globules in junctional membranes. J. Cell Biol., 57, 54.

Peracchia, C. (1973 b). Low resistance junctions in crayfish II. Structural details and further evidence for intercellular channels by freeze-fracturing and negative staining. J. Cell Biol., 57, 66.

Peracchia, C. (1977). Gap junctions. Structural changes after uncoupling procedures. J. Cell Biol., 72, 628.

Peracchia, C. (1978). Calcium effects on gap junction structure and cell uncoupling, Nature, 271, 669.

Peracchia, C. (1980). Structural correlates of gap junction permeation. Int. Rev. Ctyol., 66, 81.

Peracchia, C. and Peracchia, L. (1980 a). Gap junction dynamics: reversible effects of divalent cations. J. Cell Biol., 87, 708.

Peracchia, C. and Peracchia, L. (1980 b). Gap junction dynamics: reversible effects of hydrogen ions. J. Cell Biol., 87, 719.

Pinto de Silva, P. and Branton, D. (1970). Membrane splitting in freeze-etching. J. Cell Biol. 1970, 45, 590.

Politoff, A. and Pappas, G.D. (1972). Mechanism of increase in coupling resistance at electrotonic synapses of the crayfish septate axon. Anat. Rec., 172, 384.

Pople, J.A. (1951). Molecular association in liquids II. A theory of the structure of water. Proc. Roy. Soc. (London) A 205, 163.

Potter, D.D., Furshpan, E.J. and Lennox, E.S. (1966). Connections between cells of the developing squid as revealed by electrophysiological methods. Proc. Natl. Acad. Sci., USA, 55, 328.

Ramachandran, G.N. (1974). In Peptides, Polypeptides and Proteins (Blout, E.R., Bovey, F.A., Goodman, M. and Lotan, N., eds.). Wiley Interscience, N.Y., p. 14.

Raviola, E., Goodenough, D.A. and Raviola, G. (1980). Structure of rapidly frozen gap junctions. J. Cell Biol., 87, 273.

Ray, T.R. (1980). A modified method for the isolation of plasma membrane from rat liver. Biochim. Biophys. Acta., 196, 1.

Revel, J.P. and Karnovsky, M.J. (1967). Hexagonal array of subunits in intercellular junctions of mouse heart and liver. J. Cell Biol., 33, C7.

Reynolds, J.A. and Tanford, C. (1970 a). Binding of sodium dodecyl sulphate to proteins at high binding ratios. Possible implications for the state of proteins in biological membranes. Proc. Natl. Acad. Sci., USA, 66, 1002.

Reynolds, J.A. and Tanford (1970 b). The gross conformation of protein-sodium dodecyl sulphate complexes. J. Biol. Chem., 245, 5151.

Reynolds, J.A., Gilbert, D.B. and Tanford, C. (1974). Empirical correlation between hydrophobic free energy and aqueous cavity surface area. Proc. Natl. Acad. Sci., USA, 71, 2925.

Richardson, J.S. (1981). The anatomy and taxonomy of protein structure, Adv. Protein Chem., 34, 164.

Richmond, T.J. and Richards, F.M. (1972). Folding of α-helices. J. Mol. Biol. 119, 537.

Robertson, J.D., Zampighi, G. and Simon, S.A. (1981). Biophysical studies of mammalian lens junctions. Biophys. J., 33, 77a.

Rossmann, M.G. and Henderson, R. (1982). Phasing electron diffraction amplitudes by molecular replacement method. Acto. Cryst. Sect. A, 38, 13.

Rowe, E.S. and Steinardt, J. (1976). Electrooptical properties of reduced protein - sodium dodecyl sulphate complexes. Biochemistry, 15, 2579.

Salemme, F.R. (1981). Conformational and geometrical properties on β-sheets in proteins III. Isotrophically stressed configurations. J. Mol. Biol., 146, 143.

Salemme, F.R. and Weatherford, D.W. (1981 a). Conformation and geometrical properties of β-sheets in proteins I. Parallel β-sheets. J. Mol. Biol., 146, 101.

Salemme, F.R. and Weatherford, D.W. (1981 b). Conformation and geometrical properties of β-sheets in proteins II. Antiparallel and Mixed β-sheets. J. Mol. Biol., 146, 119.

Schlieden, M.J. (1838). Beitrage zur Phytogenesis. Mullers Arch. Anat. Physiol. Wiss. Med. 1838, 137.

Schwarzmann, C.H., Welgandt, H., Rose, B., Zimmremann, A., Ben-Haim, D., and Lowenstein, W.R. (1981). Diameter of cell-to-cell junctional channels as probed with neutral molecules. Science 213, 551.

Shapiro, A.L., Vinuela, E. and Maizel, J.V. (1967). Molecular weight estimation of polypeptide chains by electrophoresis in SDS-polyacrylamide gels. Biochem. Biophys. Res. Commun., 28, 815.

Sheridan, J.D., Hammer-Wilson, M., Preus, D., and Johnson, R.G. (1968). Quantitative analysis of low-resistance junctions between cultured cells and correlation with gap junctional areas. J. Cell Biol., 76, 532.

Sherwood, D. (1976). Crystals, X-rays and Proteins. Longman, London.

Shrager, P.C., Strickholm, A. and Macey, R.C. (1969). Chemical modification of crayfish axons by protein cross-linking aldehydes. J. Cell Physiol., 74, 91.

Shubnikov, A.V. and Koptsik, V.A. (1974). Symmetry in Science and Art. Plenum Publishing Corporation, New York.

Simpson, I., Rose, B., and Lowenstein, W.R., (1977). Size limits of molecules permeating the junctional membrane channels, Science, 195, 294.

Slayter, H.C. (1976). High resolution metal replication of macromolecules. Ultramicroscopy, 1, 341.

Sleytr, U.V. (1970). Die Gefrie ratzung korrespondierender bruchhalflen: ein neur weg xur aufklarung von membranstrakturen. Protoplasma, 70, 101.

Sleytr, U.B. and Robards, A.W. (1977). Plastic deformation during freeze-clearing: a review. J. Microsc., 110, 1.

Sleytr, U.B. and Robards, A.W. (1982). Understanding the artifact problem in freeze-fracture replication: a review. J. Microscopy, 126, 101.

Socolar, S.J. and Lowenstein, W.R. (1979). Methods for studying transmission through permeable cell-to-cell junctions. In: Methods in Membrane Biology, edited by E. Korn, New York: Plenum, 10, 121.

Spence, J.C.H. (1981). Experimental High Resolution Electron Microscopy, Clarendon Press, Oxford.

Spatz, L. and Strittmatter, P. (1971). A form of cytochyome b_5 that contains an additional hydrophobic sequence of 40 amino acid residues. Proc. Natl. Acad. Sci., USA, 68, 1042.

Spray, D.C., Harris, A.L. and Bennett, M.V.L. (1981). Glutaraldehyde differentially affects gap junctional conductance and its pH and voltage dependence. Biophys. J., 33, 108a.

Staehlin, L.A. (1968). The interpretation of freeze-etched artifical and biological membranes. J. Ultrastruct. Res., 22, 326.

Stretton, A.O.W., and Kravitz, E.A. (1973). Intracellular dye injection: the selection of Procion yellow and its application in preliminary studies of neuronal geometry in lobster nervous system, in: Intracellular Staining in Neurobiology (S.B. Kater and C. Nicholson, eds.), p. 21, Springer-Verlag, New York.

Stuhrmann, H.B. (1982). Contrast variation in small angle x-ray scattering. (Glatter, O. and Kratky, O., eds.) Academic Press, New York.

Subak-Sharpe, J.H., Burk, R.R. and Pitts, J.D. (1966). Metabolic cooperation by cell-to-cell transfer between genetically different mammalian cells in tissue culture. Heredity, 21, 342.

Subak-Sharpe, J.H., Burk, R.R. and Pitts, J.D. (1969). Metabolic communication between biochemically marked mammalian cells in culture. J. Cell Sci., 4, 353.

Tanford, C. (1974). Theory of micelle-formation in aqueous solutions. J. Phys. Chem., 78, 2469.

Tanford, C. (1968). Protein denaturation. Adv. Protein Chem., 23, 121.

Tanford, C. (1980). The Hydrophobic Effect. John Wiley and Sons, New York.

Tanford, C. and Reynolds, J.A. (1976). Characterization of membrane proteins in detergent solutions. Biochim. Biophys. Acta., 457, 133.

Tanner, M.J.A. (1979). Isolation of integral membrane proteins and criteria for identifying carrier proteins in Curr. Top. Membr. Trans. (Bronner, F. and Kleinzeller, A., eds.), Academic Press, N.Y., 12, 1.

Tewari, J.P. and Malhotra, S.K. (1978). Visualization of intrinsic proteins in cross-fractured membranes in rotary-shadowed freeze-fracture replicas. Microbios Letters, 9, 35.

Tillack, T.W. and Marchesi, V.I. (1970). Demonstration of the outer surface of freeze-etched red blood cell membranes. J. Cell Biol., 45, 649.

Trautwein, W., Kuffler, S.W. and Edwards, C. (1956). Changes in membrane characteristics of heart muscle during inhibition. J. Gen. Physiol. 40, 135.

Turin, L., and Warner, A. (1977). Carbon dioxide reversibly abolishes ionic communication between cells of early amphibian embryo, Nature, 270, 56.

Unwin, P.N.T. and R. Henderson (1975). Molecular structure determination by electron microscopy of unstained crystalline specimens. J. Mol. Biol., 94, 425.

Unwin, P.N.T. and Zampighi, G. (1980). Structure of the junction between communicating cells. Nature, 283, 545.

Vainshtein, B.K. (1964). Structure Analysis by Electron Diffraction, Pergmon Press, Oxford.

Vainshtein, B.K. (1981). Modern Crystallography, Vol. I, Symmetry of Crystals. Methods of structural crystallography, Springer Series in Solid-State Sciences, Spring-Verlag, Berlin.

Van Bueren, H.G. (1960). Imperfections in Crystals. North-Holland Publishing Company, Amsterdam. J. Gen. Physiol. 40, 135.

Van der Kloot, W.C. and Dane, B. (1964). Conduction of action potential in the frog ventricle, Science, 146, 74.

Van Harreveld, A. and Crowell, J. (1964). Electron microscopy after rapid freezing on a metal surface and substitution fixation. Anat. Rec., 149, 381.

Van Harreveld, A., Crowell, J. and Malhotra, S.K. (1965). A study of extracellular space in central nervous system by freeze-substitution. J. Cell Biol., 25, 117.

Van Venrooij, G.E.P.M., Aertsen, A.M.H.J., Wax, W.M.A., Ververgaert, P.H.J.T., Verhoeven, J.J. and Vander Vorst, H.A. (1975). Freeze-etching: freezing velocity and crystal size at different locations in samples. Cryobiology, 12, 46.

Weber, K. and Osborn, M. (1969). The reliability of molecular weight determination by dodecyl-sulphate poly-acrylamide gel electrophoresis. J. Biol. Chem., 244, 4406.

Weber, K. and Osborn, M. (1975). Proteins and sodium dodecyl sulphate: Molecular weight determination on polyacrylamide gels and related procedures. In "The Proteins", Vol. 1, (H. Neurath and R.L. Hill, eds.), Academic press, N.Y., 179.

Wehrli, E., Muhlethaler, K. and Moor, H. (1970). Membrane surface as seen with a double replica method for freeze-fracturing. Exp. Cell Res., 59, 336.

Weidmann, S. (1952). The electrical constants of Purkinje fibres, J. Physiol. London, 118, 348.

Willison, J.H.M., and Rowe, A.J. (1980). Replica, shadowing and freeze-etching techniques. In: Practical Methods in Electron Microscopy (A.M. Glauert, ed.), Vol. 8, North-Holland, Amsterdam.

Wolpert, L. (1981). Positional Information and Pattern Formation, Phil. Trans. Roy. Soc. Lond. B, 295, 441.

Wray, W., Boulikas, T., Wray, V. and Hancock, R. (1981). Silver staining of proteins in polyacrylamide gels. Anal. Biochem., 118, 197.

Yee, A.G. and Revel, J.P. (1978). Loss and reappearance of gap junctions in regenerating liver. J. Cell Biol., 78, 554.

Zampighi, G. and Unwin, P.N.T. (1979). Two form of isolated gab junctions. J. Mol. Biol. 135, 451.

Zampighi, G., Corless, J.M. and Robertson, J.D. (1980). On gap junction structure, J. Cell Biol., 86, 190.

7. APPENDIX A

7.1 On the Solubilization of Integral Membrane Proteins

Except for a notable few, most of the integral membrane proteins have thus far resisted attempts at thorough purification and characterization. This slow pace of progress in this particular field has largely been a consequence of the specialized molecular features of these integral membrane proteins which have proven difficult to isolate and characterize by employing methods that have proven so successful in the case of the water soluble proteins (Tanner, 1979; Maddy and Dunn, 1976). In the integral membrane proteins, predominantly hydrophobic surfaces are in contact with the hydrocarbon regions of the lipid bilayer, whereas the hydrophilic surfaces are exposed to the aqueous medium (Tanford, 1980). The other variants are also possible for example an integral membrane protein may be totally or partially immersed in the hydrophobic region of lipid bilayer (Folch-Pi and Stoffyn, 1972; Spatz and Strittmatter, 1971). Because of the amphiphilic nature of integral membrane proteins, their isolation and subsequent purification is fraught with problems. Since their hydrophobic regions are intimately associated with the alkyl chains of lipid bilayer by virtue of the hydrophobic effect and the polar regions may be associated with the lipid headgroups (in addition to being exposed to the aqueous environments), they would require such preferential interactions upon separation from the phospholipid bilayer. Such an environment can not be provided by either aqueous or organic solvents alone.

So the problem here is that of simulating the native environment of an integral membrane protein as an amphiphilic environment is required having a liquid hydrocarbon region of comparable dimensions bounded by polar environment (Tanford and Reynolds, 1976). The word detergent refers to a special class of lipids with amphiphilic molecules having a single alkyl chain linked to a polar head group and organize into oblate ellipsoidal micelles in aqueous solution (Tanford, 1974). In solution, their apolar moeities disrupt the interaction amongst the water molecules with very little compensating attraction between the hydrocarbon regions (apolar) and water molecules. Consequently water molecules nearest to these hydrocarbon regions are coerced into networks forming polyhedral cage like cavities attempting to enclose the solute hydrocarbon. This may not entail any breaking of hydrogen bonds, as the bond distortions (Pople, 1951; Bernal, 1964) themselves can produce the accommodating effect (Tanford, 1980). There is a concomitant reduction in the internal mobility of hydrocarbon chains (Arnow, 1963). This causes an entropy loss and hence the phenomenon is rendered thermodynamically unfavourable. According to the available experimental evidence the molar free energy for the transfer of hydrocarbons from pure liquid hydrocarbons to aqueous solution (which reflects their innate hydrophobicity) is approximately linearly related to the hydrocarbon surface area (Hermann, 1972; Reynolds et al., 1974). [The area is measured at .15 **nm** distance from the hydrocarbon surface. This is the closest distance that the centers of water molecules can get to the hydrocarbon surface.] Obviously the amphiphiles with large apolar groups are going to be more hydrophobic too.

Similarly, amphiphiles with large polar groups would be more hydrophilic.

The phospholipids (diacylphospholipids) of the membranes differ a great deal from the soluble amphiphiles (which include the detergents used for membrane protein solubilization) in possessing a less hydrophilic nature which is reflected by a low value of hydrophile-lipophile balance (Griffin, 1949), whereas the detergents employed in membrane solubilization usually have a high monomer solubility in water. Usually when a small amount of an amphiphile is dissolved in water, a part of it stays in the solution in the form of free monomers in equilibrium with the other part which form a monolayer at the air/water interface. However, if the monomer concentration rises up to a critical concentration, added amphiphiles associate to form thermodynamically stable colloidal aggregates called micelles (Helenius and Simons, 1975). This narrow range of critical concentration of amphiphiles is known as the critical miceller concentration. Yet another detergent property which is of interest in the solubilization of integral membrane proteins is the aggregation number which represents the average number of amphiphile molecules per micelle (Helenius and Simons, 1975; Tanford, 1980). It has been suggested that the detergents act upon the membranes in three steps (Helenius and Simons, 1975). Initially, detergent interacts with and gets incorporated into the phospholipid bilayer, at low concentrations. As the detergent concentration increases, bilayers saturate with the detergent leading to the creation of the mixed micells of detergents and phospholipids. After the completion of micellerization, the detergent content of the micelles

increases selectively. Concomitantly their size reduces to a minimum limiting value (Helenius and Simons, 1975). If the detergent concentration is raised any further, pure detergent micelles are formed which exist in equilibrium with the mixed micelles. In this respect it is of interest to note that the effect of lyotropic detergents may exert a pressure for increasing curvature in the bilayer on account of their "wedge" shape like structure (Haydon and Taylor, 1963) and may thus result in the generation of smaller mixed micelles. Whereas bile salts may "chop up the bilayers" into disc-like fragments with bile salt molecules lining up on the hydrophobic edges (Helenius and Simons, 1975).

Obviously if a protein is to be maintained in its optimal state it would have to have a substantial number of detergent molecules surrounding the hydrophobic part of the protein and thus simulating the environment of the bilayer core. The choice of the detergent, therefore would be influenced by the normal micelle sizes. It is known that the long hydrocarbon chain amphiphiles form disc-shaped micelles. Since the thickness of the hydrophobic region is governed by the hydrocarbon chain length, it is evident that the detergents with C_{16} and C_{18} hydrocarbon alkyl chains will be able to most closely reproduce the hydrophobic environment of the membrane (Helenius and Simons, 1975).

Since the hydrocarbon cores of the micelles of lipid bilayers are fluid in nature, the dimensions of chain lengths required for maintaining the optimal protein structure could be easily distorted by the very presence of the protein. The dimensions of the proteins hydrophobic surface would also become an important factor in governing the extent of distortion.

In some cases it has been observed that if the detergent does not strip away the phospholipids intimately associated with the proteins and instead it undergoes hydrophobic binding with them, the isolated soluble complex (of proteins, phospholipids and detergent) retains its biological activity regardless of the nature of the detergents employed, even if they resembled phospholipids only distantly (Tanford and Reynolds, 1976). Detergents are generally classified into three types, which vary in their action on the membrane proteins, namely; (i) nonionic detergents, (ii) ionic detergents and (iii) bile salts (reviewed in detail by Helenius and Simon, 1975; Tanford and Reynolds, 1976; Tanner, 1979). The nonionic detergents are the mildest types and they do not bind to soluble proteins unless they have a hydrophobic surface. Ionic detergents undergo massive cooperative binding with the soluble proteins, resulting in the protein denaturation. Bile salts are closer to nonionic detergent in their action on the soluble proteins which are usually not denatured. In case of the oligomeric proteins, the protein-protein interactions are often retained intact with bile salts (Tanner, 1979).

Detergent bind to the integral membrane proteins by incorporating them into micelles (Tanford and Reynolds, 1976), where the hydrophobic region of a protein is intercalated into the hydrophobic interior of a micelle. Non-ionic detergents would not bind to the hydrophilic regions of the proteins exposed to the aqueous environment. However, the ionic detergents would undergo strong coopertaive binding with these regions, and thus induce local protein denaturations. Bile

salts appear to behave more like non-ionic detergents in solubilization of the integral membrane proteins (Spatz and Strittmatter, 1971).

Nevertheless it must be clear that no detergent is entirely capable of simulating the environment present in the biomembranes, and in some cases loss of biological activity has been reported with bile salts and even nonionic detergents (Medzihradsky et al., 1967).

8. APPENDIX - B

8.1 Theoretical Basis of the Determination of Molecular Weight by SDS-Page

Interaction of SDS and Proteins

The potent solubilizing action of SDS on membrane proteins and proteins in general stem from its ability to dissociate proteins into constituent polypeptides and protein-lipid complexes into proteins and lipids. Therefore the molecular weight dependent separation of polypeptide chains is easily achieved by running polyacrylamide gel electrophoresis in the presence of SDS. It is the free monomeric concentration of detergent that governs the amount of detergent bound to the protein. The association of anionic long-chain amphiphiles like SDS with proteins has a great affinity (and results in increased binding) than of cationic and non-ionic detergents and bile salts. SDS undergoes massive cooperative binding with virtually all the proteins, accompanied by drastic changes in optical and hydrodynamic characteristics reflecting major conformational changes (Reynold and Tanford, 1970 b). It has been established that the maximum amount of SDS that is bound per gram of protein is nearly the same for all of them (Reynolds and Tanford, 1970 a,b). Detergent binding to these proteins (without disulfide bonds or with disulfide bonds reduced when present in the native state) results in actually two types of the complex, one consisting of 0.4 gm dodecylsulphate per gm protein (one amphiphile

per seven amino acid residues), and the other having 1.4 gm dodecylsulphate per gm protein (one amphiphile per two amino acid residues). The transition between the two forms occurs at 6 to 7 x 10^{-4}M dodecylsulphate at 25°C, pH 5.6 to 7.2 with only slight dependence on the ionic strength (Reynolds and Tanford, 1970 a). All proteins are dissociated into the constituent polypeptide chains and each SDS-polypeptide complex assumes the shape of an extended rod (prolate ellipsoid) particle with constant short axis of the order of 1 nm and the long axis varying in length with the molecular weight (Reynolds and Tanford, 1970 b). This particle may have short rod-like segments with some flexible intervening regions (Rowe and Steinnardt, 1976). The protein is in a form of a denatured state which displays a substantial fraction of polypeptide chains in an α-helical organization. It is comprised of several lengths of helical polypeptide chains intervened with flexible joints. This disposition facilitates the exposure and subsequent association of most of the hydrophobic side chains to a large number of hydrophobic ligands per molecule. The gain in free energy achieved by the binding of hydrophobic ligands with the hydrophobic groups may be significantly greater than the unfavourable free energy change associated with the accompanying conformational change, and therefore the transition to the altered conformational state would be favourably induced by the binding of the ligand (Tanford, 1968). Very similar complexes are formed in the case of proteins with intact disulphide bridges, restricted only by the steric limitations posed by the disulphide bridges. However, the detergent binding is slightly reduced

and consequently the resulting complex is not linearly as extended (Fish et al., 1970).

The extent of association between the dodecyl-sulphate and proteins depends on the molecular weight of proteins. Since in these complexes the effect of native protein charges is swamped by the SDS charge, therefore all the protein complexes would have a uniform charge: mass ratio. The mobility of polypeptides on the gel would be governed by both, the molecular charge, and the sieving through the gel pores. Since these complexes are of uniform shape (rod-like), they would separate in gel electrophoresis strictly on the basis of molecular weight. However, even for water soluble proteins, the binding of the detergent is slightly governed by the amino acid composition of the protein. It appears that the basic proteins undergo slightly more binding with the detergent in comparison to the acidic proteins. Therefore the apparent molecular weights derived by measuring electrophoretic mobilities should be regarded more appropriately as only approximates.

Electrophoretic Mobility

If a particle in a fluid with a net charge is subjected to the influence of an applied electric field, the particle will be induced to move under the electric force exerted on it. This force is a function of both the strength of the field **E** and the charge on the particle **q** and is given by

$$\mathbf{Fel} = \mathbf{qE} \qquad \ldots\ldots\ldots (1)$$

However as the particle moves, the surrounding fluid medium would apply a frictional retarding force on it. This force would be governed by the fluid and the geometry of the particle in question. But in general it is usually presumed that the frictional force is proportional to the particle's velocity or

$$Ffr = fV \qquad \ldots\ldots\ldots (2)$$

where **f** denotes a constant of proportionality called the frictional coefficient. The particle will accelerate, but only for a short duration when the electric potential is first applied. It will rapidly attain an equilibrium velocity where the driving electrical force becomes equal to the retarding frictional force because at equilibrium Newton's second law of motion states the sum of forces acting on a body in equilibrium add up to zero (Gabler, 1978). Since the motion is always counteracted by frictional forces, the two forces can be equated. At equilibrium we have,

$$fV = qE \qquad \ldots\ldots\ldots (3)$$

or

$$M = \frac{V}{E} = \frac{q}{f} \qquad \ldots\ldots\ldots (4)$$

where the ratio $\frac{V}{E}$ represents the electrophoretic mobility, defined as particles velocity per unit field. Indeed it is a physical parameter representative of a molecule under the conditions in which it was evaluated. It is a function of the molecule's charge and also of its geometric configuration as different shapes would cause different frictional drags. The net charge, however, is dependent on the pH, and possibly on the temperature and the solvent too.

In case of a sherical particle, it can be demonstrated that $f = 6\pi\eta_v r$ (5) where η_v is the viscosity of the solvent and r corresponds to the radius of the sphere. For other geometries, the frictional coefficient can be similarly derived, but it is mathematically less tractable. It is evident from the definition of mobility that its units are square centimeters per volt second. For typical globular proteins M usually range between 0.1×10^{-4} and 1.0×10^{-4} cm^2/V sec; whereas for small univalent ions M takes on the values around 6×10^{-4} cm^2/V sec.

The above described simplified account of electrophoretic mobility permits one to gain a broad understanding of those factors that may influence it. However it can not be employed for any detailed analysis because a number of problems crop up. The effect of counterion layer surrounding the particle (that attenuates the applied field at the charged particle) and its distortion due to shear when the particle moves through the fluid under the influence of the applied field have not been accounted for.

Estimation of molecular weight

Based upon studies with native proteins on starch and polyacrylamide gels (Ferguson, 1964; Hendrick and Smith, 1968) in buffer solutions, it has been demonstrated that molecular weights of proteins can be measured if relative mobalities (m_R) are available at several gel concentrations. The relationship between the relative mobility m_R and molecular weight is described by the Ferguson equation.

$$\text{Log } m_R = -K_R C + \text{Log } m_o \quad \ldots\ldots\ldots (6)$$

where m_R is the relative mobility at gel concentration C, m_o is the relative mobility at zero gel concentration ("apparent free relative mobility") and K_R is the "retardation coefficient'. K_R is governed by the degree of cross-linking in the gel system, the shape of the molecules and their molecular weights (Weber and Osborn, 1975). That several proteins can be treated by such an approach was first demonstrated by Hendrick and Smith (1968). They have outlined a simple approach for the estimation of molecular weights of globular proteins on polyarcylamide gels. Plotting the $\log_{mR}$ values of standard proteins against the various known gel concentrations gave straight lines with slopes of $-K_R$ ("Ferguson plots"; Ferguson, 1964). Replotting K_R values against the molecular weight yielded linear relationship which could be exploited to obtain the molecular weights of the unknown proteins. The "apparent free mobility", m_o, is dependendent upon the protein and on its inherent charge, shape, and size. A plot of electrophoretic mobilities of various proteins against the gel concentration (Ferguson plot) reveals that all the straight lines in the plot intersect at approximately the same value for zero gel concentration (Neville, 1971). The fact that m_o occupies a nearly constant value in the SDS system is demonstrative of a linear relationship between Log m_R and K_R, empirically established (Shapiro et al., 1967; Weber and Osborn, 1969) at any given gel concentration. Therefore, if the shape factor and degree of cross-linking can be considered as constants, Log m_R is a linear function of molecular weight. In Ferguson plots, there is however a small variation in the value of m_o

that is greater than can be accounted for due to experimental error (Neville, 1971). The source of this variation lies with the individual characters of protein species. For example, glycoproteins that behave atypically on the Ferguson plots can be readily diagnosed.